Aerosol-radiation interactions in China in winter: Competing effects of reduced shortwave radiation and cloud-snowfall-albedo feedbacks under rapidly changing emissions

Jonathan M. Moch[1,2], Loretta J. Mickley[1], Christoph A. Keller[3,4], Huisheng Bian[3,4], Elizabeth W. Lundgren[1], Shixian Zhai[1], Daniel J. Jacob[1,2]

[1] John A. Paulson School of Engineering and Applied Sciences, Harvard University, Cambridge MA, USA

[2] Department of Earth and Planetary Sciences, Harvard University, Cambridge, MA, USA

[3] Global Modeling and Assimilation Office, NASA Goddard Space Flight Center, Greenbelt, MD, USA

[4] Universities Space Research Association, Columbia, MD, USA

Key Points:

- GEOS-Chem aerosols are for the first time coupled to radiation in an Earth System Model to examine aerosol radiation interactions in China
- Absorbing aerosols aloft can reduce clouds and snowfall, causing more surface absorption of radiation despite aerosol reflection aloft
- Aerosol radiation interactions over China in winter can increase surface particulate matter concentrations by ~10-20%

Abstract:

Since 2013, Chinese policies have dramatically reduced emissions of particulates and their gas-phase precursors, but the implications of these reductions for aerosol-radiation interactions are unknown. Using a global, coupled chemistry-climate model, we first examine how the radiative impacts of Chinese air pollution in the winter months of 2012 and 2013 affect local meteorology and how these changes may, in turn, influence surface concentrations of $PM_{2.5}$, particulate matter with diameter less than 2.5 μm. We then investigate how decreasing emissions through 2016 and 2017 alter this impact. We find that absorbing aerosols aloft in winter 2012 and 2013 heat the mid- and lower troposphere by ~0.5-1° C, reducing cloud liquid water, snowfall, and snow cover. The subsequent decline in surface albedo counteracts the ~15-20 W m^{-2} decrease in shortwave radiation reaching the surface due to attenuation by aerosols overhead. The net result of this novel cloud-snowfall-albedo feedback in winters 2012-13 is a slight increase in surface temperature of ~0.5-1° C in some regions and little change elsewhere. The aerosol heating aloft, however, stabilizes the atmosphere and decreases the seasonal mean planetary boundary layer (PBL) height by ~50 m. In winter 2016 and 2017, the ~20% decrease in mean wintertime $PM_{2.5}$ weakens the cloud-snowfall-albedo feedback, though it is still evident in western China, where surface temperatures warm by ~0.5-1° C. Regardless of emissions, we find

that aerosol-radiation interactions enhance mean surface $PM_{2.5}$ pollution by 10-20% across much of China during all four winters examined, mainly though suppression of PBL heights.

Plain Language Summary:

Particulate matter, also called aerosols, influences climate through the absorption and reflection of solar radiation traveling through the atmosphere. Trends in particulate matter can therefore impact local and regional climate, which may in turn exacerbate particulate pollution. Here we embed a detailed atmospheric chemistry scheme within a global climate model to examine aerosol-radiation interactions and their impact on particulate pollution over China in winter 2012-2013 and 2016-2017. We find that surface particulates decrease by 20% between the time periods, a result of stricter regulations. In both time periods, aerosol absorption of sunlight heats the atmosphere aloft, leading to more stable conditions. This in turn amplifies the concentration of surface particulate pollution by 10%-20%, again in both time periods. Aerosol heating aloft also diminishes cloud cover, which then reduces snowfall, especially in 2012-2013. The subsequent loss of snow cover allows more sunlight to warm the surface, counteracting to some extent the surface cooling from reflection of sunlight by aerosols aloft. This work suggests an important role for absorbing aerosols like soot in affecting local climate; it also demonstrates the potential for climate models with detailed chemistry to shed new light on interactions between aerosols and climate.

1 Introduction:

Fine particle pollution ($PM_{2.5}$, particulate matter with diameter less than 2.5 μm) is responsible for over 1-2 million deaths per year in China (Cohen et al., 2017; Vohra et al., 2021). In addition to this significant impact on public health, $PM_{2.5}$ – the fine component of the aerosol – affects climate both directly, by influencing how radiation traverses the atmosphere, and indirectly, through its interactions with clouds (Myhre et al., 2013). Given the high aerosol burden over China, changing $PM_{2.5}$ concentrations can strongly influence anthropogenic radiative forcing, temperature trends, and regional meteorology (Liao et al., 2015; K. Li et al., 2016; Miao et al., 2019). Between 2013 and 2018, China enacted a series of policies aimed at reducing $PM_{2.5}$, and surface observations show a dramatic reduction of annual mean $PM_{2.5}$ across China by ~30-50% during this period, resulting in large part from these policies (Zhai et al., 2019; Zhang et al., 2019).

Attribution of the decline in $PM_{2.5}$ to emissions reductions is complicated, however, by the variability in meteorology, which can also influence $PM_{2.5}$ concentrations on interannual, seasonal, and daily timescales (Leung et al., 2018; Zhai et al., 2019), as well as on local and synoptic spatial scales. Additionally, quantifying the effect of meteorology on $PM_{2.5}$ abundance in China is made difficult by the feedback of $PM_{2.5}$ onto regional and local meteorology, so that some meteorological variation may actually be driven by emission changes. Aerosol-radiation and aerosol-cloud interactions may thus promote extreme haze events, during which $PM_{2.5}$

concentrations can exceed 200 μg m^{-3} (Ding et al., 2016; Miao et al., 2019). Using a global, coupled chemistry-climate model, we examine the effect of changing aerosol concentrations on both local and regional climate in China, thereby shedding light on the magnitude of aerosol-radiation feedbacks in the region and the value of emission reduction policies for $PM_{2.5}$ reductions. We focus here only on aerosol-radiation interactions.

By reflecting and absorbing light that otherwise would have reached the Earth's surface, aerosols alter the radiation balance of the atmosphere. Aerosol optical depth (AOD) in China frequently nears or exceeds one, especially during heavy haze events (Li et al., 2013; Che et al., 2014; Che et al., 2015; Zhang et al., 2020). Such events are usually characterized by a significant presence of absorbing aerosols (Xie et al., 2015; Xia et al., 2016). The high levels of absorbing and scattering aerosols lead to a substantial aerosol direct radiative effect, reducing the downward solar flux at the surface and increasing radiation absorbed within the atmosphere (Xia et al., 2016; Li et al., 2017; Zhong et al., 2018b). For example, during a haze event in Beijing in January 2013, Bi et al. (2014) estimated that about half the incoming solar radiation went into heating the atmosphere instead of the surface.

Such changes in the radiation balance due to the presence of aerosols may lead to a cascade of meteorological effects, including cooling at the surface and warming at the top of the planetary boundary layer (PBL) or just above it (Li et al., 2017; Huang et al., 2018; Miao et al., 2019). Of chief importance for $PM_{2.5}$ pollution is the potential decrease of PBL height. By reducing temperatures at the surface and increasing temperatures aloft, aerosols can increase the thermal stratification of the PBL, suppressing vertical mixing and thereby reducing PBL height (Ding et al., 2016; Huang et al., 2018; Miao et al 2019). Greater stratification of the PBL can also weaken surface wind speeds by impeding the vertical flux of horizontal momentum from higher altitudes to the surface (Jacobson and Kaufman, 2006; Gao et al., 2015; Zhong et, al 2018b). Cooler surface temperatures, in turn, can increase relative humidity (RH, Liu et al., 2018; Zhong et al., 2018a). Finally, aerosol-radiation interactions can suppress precipitation locally by reducing surface evaporation and convection, while at the same time enhancing precipitation downwind of polluted areas (Fan et al., 2015; Li et al., 2017; Liu et al., 2018). Warmer temperatures aloft due to absorbing aerosols can also limit cloud formation and subsequent precipitation (Fan et al., 2015; Liao et al, 2015). Aerosols can also indirectly affect cloud formation by acting as cloud condensation nuclei, which can increase the concentration but limit the size of cloud droplets. These changes enhance cloud albedo but decrease precipitation (Lohmann and Feichter, 2004; Liao et al., 2015). On a synoptic scale, observations and models suggest that aerosols can change large-scale circulation patterns, such as by weakening of the East Asian monsoonal circulation (Zhang et al., 2012; Z. Li et al., 2016; Jiang et al., 2017; Niu et al., 2018; Liu et al., 2019).

These aerosol-radiation interactions may lead to meteorological feedbacks that alter $PM_{2.5}$ concentrations. Across China, $PM_{2.5}$ abundance is strongly influenced by temperature, PBL height, wind speed, RH, and precipitation (Leung et al., 2018; Zhai et al., 2019). In general,

shallower PBL heights are associated with higher levels of surface $PM_{2.5}$ since the PBL governs the volume of air into which surface emissions can mix (Li et al., 2017; Miao et al., 2019). Low wind speeds are similarly associated with higher $PM_{2.5}$ concentrations due to the decrease in ventilation (Jacob and Winner, 2009; Ji et al., 2014). Precipitation provides a major sink for $PM_{2.5}$ through wet deposition, and reductions in local rainfall can therefore increase $PM_{2.5}$ (Chen et al., 2018; Leung et al., 2018). RH in the PBL is generally positively correlated with $PM_{2.5}$ in northern China, probably because higher RH in this region is strongly related to declines in PBL height and to the water content of clouds and aerosol, which in turn is linked to the chemical production of $PM_{2.5}$ (Leung et al., 2018; Zhai et al., 2019; Moch et al., 2018; Liu et al., 2018; Shao et al., 2019). However, in southern China, RH is usually negatively correlated with $PM_{2.5}$, possibly because here RH is more strongly associated with precipitation and the southerly airflow that can ventilate the region. Surface temperatures in China are positively correlated with $PM_{2.5,}$ but this may be partly a result of the relationships between temperature and other meteorological variables such as stagnation (Leung et al, 2018; Zhai et al., 2019). At the regional scale, a weaker East Asian winter monsoon is associated with higher levels of $PM_{2.5}$ in East Asia (Cai et al., 2017; Wang et al., 2019).

Many of the meteorological conditions that promote particulate pollution are the same as those that aerosol-radiation interactions enhance, and so these interactions may act as a positive feedback for $PM_{2.5}$. For example, the PBL feedback exacerbates levels of $PM_{2.5}$ (Quan et al., 2014; Zheng et al., 2015; Miao et al. 2019) and increased $PM_{2.5}$ may further weaken the East Asian monsoon circulation and decrease wind speeds (Wu et al., 2016). Indeed, evidence of aerosol-radiation interactions driving $PM_{2.5}$ pollution has been inferred from observations for multiple regions in China (e.g., Huang et al., 2018; Zhong et al., 2019). For example, such interactions may have enhanced the effectiveness of the brief dramatic reductions in emissions in Beijing in November 2014, when the Asia-Pacific Economic Cooperation Conference took place and strict air quality measures were enacted (Gao et al., 2017; Zhou et al., 2019).

Multiple modeling studies have shown that accounting for the direct aerosol-radiation feedbacks is critical for accurate simulation of both pollution concentrations and meteorological conditions of extreme haze episodes (Gao et al., 2015; Miao et al., 2016; Qiu et al., 2017; H. Wang et al., 2018; X. Wang et al., 2018). In general, these prior studies have examined individual haze events in particular locations using regional models with prescribed boundary conditions (e.g., J. Wang et a., 2014; X. Wang et al., 2018; Qiu et al., 2017). In this way, high spatial resolution over the area of interest is achieved. A typical approach is to perform two simulations, one in which aerosols influence radiation and one in which this aerosol effect is turned off. By comparing these simulations, such studies can then estimate the importance of aerosol-radiation feedbacks for $PM_{2.5}$ concentrations and meteorology during the individual event.

A key shortcoming of such studies, however, is that such feedbacks may be partially dampened by the meteorological boundary conditions used to set up the model domain. Such

boundary conditions also generally preclude the possibility of simulating aerosol-induced changes in large scale circulation patterns. The studies also typically focus on just a few days or weeks and so may not capture aerosol-radiation interactions occurring on seasonal timescales (e.g., Gao et al., 2015; H. Wang et al., 2018). In addition, examination of just one model year or season provides limited information on the feedbacks, which may vary depending on background meteorology. On the other hand, studies using Earth System Models (ESMs) to examine the effect of Chinese aerosols on climate have frequently been limited by simple representations of chemistry that may not accurately reflect the magnitude of the aerosol burden over China or the processes behind it (e.g., Liu et al., 2019; Jiang et al., 2017; Bartlett et al., 2018; Lin et al., 2018).

Our work builds upon previous studies by applying an ensemble of global model simulations to investigate the effect of emissions reductions in China on aerosol-radiation interactions for winters in four years – 2012, 2013, 2016, and 2017. We focus on winter because it has the highest $PM_{2.5}$ concentrations among other seasons in China, and therefore the largest impacts on regional climate and meteorology. Using an ESM with two-way coupling to the GEOS-Chem atmospheric chemistry model, we shed light on the role of aerosol-radiation feedbacks in influencing observed trends of $PM_{2.5}$ in China. Previous work has coupled GEOS-Chem to the regional Weather Forecasting Model (WRF) for study of aerosol-meteorology coupling (Feng et al., 2021), but our work represents the first time that GEOS-Chem aerosols have been fully coupled with the radiation scheme in an ESM. The heavy but rapidly changing aerosol burden over China provides a good case study for examining the importance of aerosol-radiation feedbacks using this new model setup. We focus here only on aerosol-radiation interactions, and do not consider aerosol indirect effects involving cloud condensation nuclei. By quantifying the possible enhanced effectiveness of emissions reductions due to aerosol-radiation feedbacks, our work provides guidance for designing and evaluating future air quality policies in China or elsewhere.

2 Methods

To examine aerosol-radiation interactions in China, we couple the aerosol emissions, chemistry, and deposition schemes from GEOS-Chem with the radiation scheme in the GEOS-ESM. In this section we describe the components of this coupled model and the simulations applied. The observations and reanalysis products used for model validation are described in the supplement.

2.1 GEOS-ESM

The Goddard Earth Observing System ESM (GEOS-ESM) is developed by the Global Modeling and Assimilation Office (GMAO) at the NASA Goddard Space Flight Center. GEOS-ESM is used for forecasts and reanalysis products such as GEOS-S2S-2 and MERRA-2 (Gelaro et al., 2017; Molod et al., 2020). GEOS-ESM has also been used for longer term prediction (e.g., decadal time scales) and in model intercomparison projects such as CMIP5 and CCMI (Ham et

al., 2014; Morgenstern et al., 2017). We briefly describe key aspects of the model in the supplement (S1). Detailed documentation of GEOS-ESM can be found elsewhere (e.g., Rienecker et al., 2008; Molod et al., 2012, 2015; Nielsen et al. 2017).

The Goddard Chemistry, Aerosol, Radiation, and Transport model (GOCART) is the default aerosol chemistry module online in GEOS-ESM (Chin et al, 2000; Chin et al., 2002; Colarco et al., 2010), providing aerosol mass to the radiation code, which then uses the mass concentrations to calculate aerosol optical depth and the impacts on absorption and scattering of shortwave and longwave radiation throughout the atmosphere. More details on GOCART are in the supplement (S1).

2.2. GEOS-Chem

GEOS-Chem is a grid-independent global/regional atmospheric chemistry model including a detailed aerosol-oxidant chemical mechanism coupled to emissions, deposition and transport (Park et al., 2004; Pye et al., 2009; Alexander et al., 2012; Sherwin et al., 2016; Travis et al., 2016). The model includes a stand-alone, grid-independent chemical module applying local operations (chemistry, emissions, deposition) on individual atmospheric columns, coupled to transport modules applying advection, convection, and boundary layer turbulence (Long et al., 2015). The standard application of GEOS-Chem is as an off-line chemical transport model (CTM) using archived meteorological data from GEOS-ESM analyses. However, the stand-alone chemical module can also be coupled to a meteorological model for on-line simulations in which the meteorological model handles the chemical transport. GEOS-Chem has been coupled in this manner to the GEOS-ESM (Hu et al., 2018), to the Beijing Climate Center ESM (Lu et al., 2020), and to WRF (Lin et al., 2020; Feng et al., 2021).

GEOS-Chem as a CTM has been used for numerous studies examining $PM_{2.5}$ and its components over China including evaluation with observations and analysis of aerosol chemistry (e.g., Shao et al., 2019; Dang et al., 2019; Zhai et al., 2021). The more complex chemical mechanism in GEOS-Chem allows for a better representation of aerosol processes over China than that provided by GOCART, which uses prescribed fields for many chemically active gas-phase species. In model comparisons with observed satellite AOD over China, GEOS-Chem tends to outperform GOCART (e.g., Cheng et al., 2012; S. Li et al., 2016).

The model as used here (version 12.7.0, https://doi.org/10.5281/zenodo.3634864) includes bulk representations of sulfate-nitrate-ammonium (SNA) aerosol, organic aerosol (OA), and black carbon (BC), dust in four size classes, and sea-salt aerosol in two size classes. Sulfate and nitrate chemistry are as described by Alexander et al. (2012) and Shah et al. (2020), and SNA thermodynamics follow ISORROPIA II (Fontoukis and Nenes, 2007). Sulfate and nitrate are also produced in sea-salt aerosol (Alexander et al., 2005). BC and OA in GEOS-Chem are divided into hydrophilic and hydrophobic fractions (Pye et al., 2009; Q. Wang et al., 2014). In addition to primary OA, we use a simple scheme for secondary organic aerosol (SOA), which

applies a fixed SOA yield from reactions of precursor gases (Pai et al., 2020). Aerosols are removed by wet and dry depositions following Liu et al. (2001) and Zhang et al. (2001), with additional formulations for BC scavenging (Q. Wang et al., 2014), wet deposition updates by Luo et al. (2019), and deposition of HNO_3 to snow (Jaegle et al., 2018). Here we have modified version 12.7.0 to include hydroxymethanesulfonate (HMS) aerosol chemistry and revised the cloud water pH calculation for in-cloud processes (Moch et al., 2018, 2020).

Global anthropogenic emissions are from the Hemispheric Transport of Air Pollution (HTAP; Janssens-Maenhout et al., 2015) inventory for 2010. Over China, the HTAP emissions are overwritten by the Multi-resolution Emission Inventory for China (MEIC; Zheng et al., 2018) for 2012-2017, which takes into account recent Chinese government interventions to reduce emissions. Open fire emissions are from the Global Fire Emissions Dataset (GFED; van der Werf et al., 2017), and biogenic volatile organic compound (VOC) emissions follow the Model of Emissions of Gases and Aerosols from Nature (MEGAN, Guenther et al., 2012). Dust and sea salt aerosols emissions are described as functions of wind speed and particle size (Farilie et al., 2010; Jaegle et al., 2011). Anthropogenic dust is added to the smallest dust size bin (i.e., diameter less than 1 μm), following Philip et al. (2017).

2.3 Coupling GEOS-Chem and GEOS-ESM

Previous implementation of GEOS-Chem within GEOS-ESM has relied on one-way coupling, in which chemical species are transported by the meteorological model but do not influence meteorology (Long et al., 2015; Hu et al., 2018; Keller et al., 2021). Here we expand on this work by implementing two-way coupling of GEOS-Chem with GEOS-ESM via connection of GEOS-Chem aerosols to the GEOS-ESM radiation scheme. This setup allows examination of rapid interactions between chemistry and dynamics, such as that occurring during pollution episodes in China. At every model time step in the GEOS-ESM, we apply boundary layer mixing and update the GEOS-Chem emissions and deposition before calculating chemical production and loss processes. In this way, we avoid excess removal of pollutants via dry deposition (Hu et al., 2018). The GEOS-ESM convection module does not account for chemical scavenging by precipitation, and therefore we use the GEOS-Chem convection scheme (Wu et al., 2007) driven by local GEOS-ESM mass fluxes (Hu et al., 2018). Using the GEOS-Chem convection scheme does not introduce significant errors in transport relative to using the GEOS-ESM scheme (Yu et al., 2018).

The connection of GEOS-Chem aerosols to the radiation code in GEOS-ESM is done by replacing the default GOCART aerosol mass with GEOS-Chem aerosol mass. Aerosol optical properties in GEOS-ESM are not altered. The method of mass replacement varies by aerosol species. For BC, OA, and ammonium, we simply overwrite the GOCART aerosol mass with that from GEOS-Chem. We also overwrite GOCART sulfate with the sum of sulfate plus HMS from GEOS-Chem. We treat HMS as having the same molecular weight as sulfate, which approximates how HMS may be misinterpreted in observations (Moch et al., 2020). For dust and

sea salt aerosol, we partition aerosol mass by size. The four smallest size bins for dust have the same bounds in GEOS-Chem and GOCART, so we simply replace the GOCART aerosol mass in each bin with that from GEOS-Chem. GOCART has an additional fifth size bin, which represents dust aerosol with particle radii > 6 μm. Given that aerosol of this size settles quickly and has minimal effect on radiation, we set the mass in this size bin to zero for this study. For sea salt aerosol, we remap the sea salt aerosol mass concentrations from the two size bins in GEOS-Chem onto the GOCART size bins, assuming that GEOS-Chem sea salt aerosol is lognormally distributed with a fine and coarse mode and thus preserving total sea salt aerosol mass (Kodros and Pierce, 2017). Finally, GEOS-Chem treats sea salt nitrate separately from other forms of nitrate, while GOCART partitions all nitrate into three size bins. We first replace the smallest nitrate size bin in GOCART with non-sea salt nitrate from GEOS-Chem. We next partition the GEOS-Chem sea salt nitrate into coarse and fine fractions based on the ratio of coarse-to-fine sea salt in each grid box. The fine and coarse fraction of sea salt nitrate of GEOS-Chem is then remapped onto the three size bins of GOCART nitrate.

2.4 Simulations overview

Each simulation we conduct employs a c90cubed sphere (~1^o x 1^o) horizontal resolution, with 72 layers in the vertical. Two main types of simulations are performed. For the first type, GEOS-Chem aerosols are linked to the radiation scheme, allowing online feedbacks between aerosols and meteorology (GEOS-GC). For the second type, we again connect GEOS-Chem aerosols to GEOS-ESM radiation, but make the aerosols over China transparent to solar radiation (GEOS-GC-China0). To accomplish this, we multiply the aerosol mass sent to the radiation code by a mask, built on a global 1° x 1° grid that zeros out aerosol mass within the geographic boundaries of China and applies a gradient in aerosol mass moving outward from these boundaries. For those grid boxes at the border adjacent to the zeroed-out boxes, we assign a value of 0.1. For each grid box adjacent to a 0.1 grid box and not already given a value, we assign a value of 0.2. We repeat this procedure outward from the borders until we reach a value of 1.0. All other grid boxes across the globe are assigned a value of 1.0. We apply this mask to all aerosol species except for dust and sea-salt, as most dust and all sea-salt are derived from natural sources. Setting up the mask in this way allows us to avoid a sharp gradient in aerosol mass, which would affect meteorology in ways different from what might be expected from gradual removal of anthropogenic emissions.

By comparing these two types of simulations, GEOS-GC and GEOS-GC-China0, we can assess the role of aerosol-radiation interactions driven mainly by pollution within China. In GEOS-GC, two-way coupling between aerosols and radiation is allowed, while in GEOS-GC-China0 the meteorology influences $PM_{2.5}$ concentrations but aerosols over China do not affect radiation. Conducting simulations with anthropogenic emissions over China turned off would offer an alternative way to capture the effect of aerosols on regional climate and meteorology (e.g. Y. Wang et al., 2014; Jiang et al., 2017), but this approach would not allow us to quantify the subsequent feedback of meteorology onto air quality. Another possible approach would be to

zero out globally all aerosol mass sent to the radiation scheme. This approach has the benefit of being globally consistent, but a major drawback would be that it could highlight the impact of non-Chinese aerosols on large-scale circulation patterns, which in turn could influence air quality in China. For example, we found previously that aerosols over Russia can perturb the Siberian High, a driver of weather and air quality in China (Moch, 2020). We therefore settle on the gradient masking approach as the one that most closely captures the effects of aerosol-radiation interactions on $PM_{2.5}$ concentrations within China.

To examine the effect of changing emissions on aerosol-radiation feedbacks over China, we perform each simulation type for two 2-year periods, 2012-2013 and 2016-2017. Observed $PM_{2.5}$ decreased by 30-40% across much of China between 2013 and 2017 in response to decreases in emissions (Zhai et al., 2019; Zhang et al., 2019). These two time windows can thus provide information on whether the magnitude and sign of the feedbacks change as emissions and surface $PM_{2.5}$ concentrations change. For each time period we prescribe the same sea surface temperatures (SSTs) as those used for MERRA-2 assimilated meteorology (Gelaro et al., 2017).

For each simulation type and each time period, we perform 5-member ensemble simulations to account for internal model variability in aerosol-radiation feedbacks. To initialize each simulation, we start with January 1 conditions from a 20-year freely running GEOS-ESM simulation with c90 horizontal resolution and 1992-2011 specified SSTs. A one-year spin-up of the model with GEOS-Chem online is carried out as follows. We first simulate 11 months in freely running mode, using emissions and specified SSTs from 2011 for the first time period and from 2015 for the second time period. The spin-up allows the longer lived species in GEOS-Chem to adjust to the appropriate meteorology. In the final month of spin-up with GEOS-Chem, the model is nudged to MERRA-2 assimilated meteorology in order to set the atmosphere to a realistic state (Orbe et al., 2017). Each of the five ensemble members is nudged by MERRA-2 meteorology from a different year, thus generating five different sets of initial conditions for the subsequent two-year simulation periods. We return the model to freely running mode for the final two years, thus allowing two-way interaction between the meteorology and aerosols to take place. We apply 2012-2013 emissions and SSTs for the first time period and 2016-2017 emissions and SSTs for the second time period. Differences between the two ensembles of simulations, while influenced in part by the SSTs applied, will also reveal how aerosol-radiation feedbacks over China have changed in response to the steep decline in emissions.

To test for statistical significance of our findings, we conduct either paired t-tests on the differences between the GEOS-GC and GEOS-GC-China0 results in each grid box or pooled t-tests for the simulation differences for each ensemble member across the two time periods. For paired t-tests, we pair the simulations by the year used to generate initial conditions. We also account for serial autocorrelation within each ensemble member, which could bias tests for statistical significance (Mickley et al., 2012). For the threshold of statistical significance, we use a p-value of less than 0.05. Grid boxes that do not meet this threshold are presented as having zero difference.

Finally, to characterize possible biases in meteorology arising in the freely running GEOS-GC simulations, we compare the GEOS-GC meteorological fields with MERRA-2 (Figure S1). To further assess model biases, we compare our results with those from the GEOS-Chem chemical transport model (GC-offline) driven by MERRA-2 assimilated meteorology (Figure S2, Zhai et al., 2021).

3 Results

We first show simulated wintertime $PM_{2.5}$ concentrations for the two time periods. We next describe the effect of aerosol-radiation interactions on meteorology and surface $PM_{2.5}$ for winter 2012-13. We then examine how changing emissions between 2012-13 and 2016-17 alter the impact of aerosol-radiation interactions between these two periods. Comparisons of GEOS-GC with GC-Offline and with MERRA-2 are included in the supplemental section (S2, Figures S1 and S2).

3.1 Simulated $PM_{2.5}$ concentrations in winters 2012-13 and 2016-17

For winter 2012-13, GEOS-GC simulates mean winter surface $PM_{2.5}$ concentrations of ~150-200 μg m^{-3} for much of eastern China (Figure 1a). In this first time period, $PM_{2.5}$ concentrations show a local maximum over the Sichuan Basin, indicated by the larger box in Figure 1a, where mean $PM_{2.5}$ levels approach 250 μg m^{-3}. Simulated $PM_{2.5}$ for the Beijing region, indicated by the smaller box, ranges from ~125-175 μg m^{-3}. We find that surface $PM_{2.5}$ concentrations simulated by GEOS-GC decrease by ~20-40 μg m^{-3} (~20%) across eastern China between 2013-12 and 2016-17 as emissions decline (Figure 1), a trend similar in magnitude to the observed decrease of ~10-50 μg m^{-3} in surface $PM_{2.5}$ in this region between 2013 and 2018 (Zhai et al., 2019). Simulated $PM_{2.5}$ across much of eastern China in winter 2016-17 thus averages ~125 μg m^{-3}, with $PM_{2.5}$ concentrations approaching ~175 μg m^{-3} in the Sichuan Basin (Figure 1b).

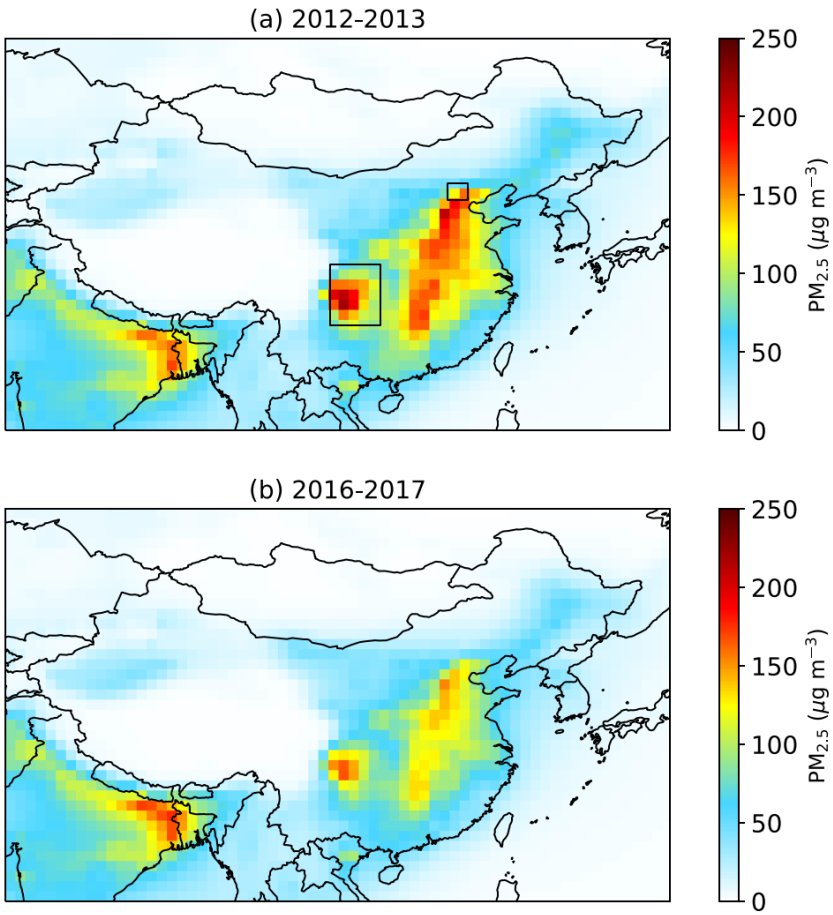

Figure 1: Simulated surface $PM_{2.5}$ concentrations for December-January-February (DJF) in GEOS-GC for (a) 201213 and (b) 2016-17. In the top panel the larger box over central China shows the location of the Sichuan Basin while the smaller box in northeastern China shows the location of Beijing municipal region.

3.2 Effect of aerosol-radiation interactions on meteorology and surface $PM_{2.5}$ in winter 2012-13

The net impact of aerosol-radiation interactions on $PM_{2.5}$ concentrations and meteorology is a combination of changes across different spatial scales. We first examine local changes and then focus on regional-scale changes in circulation patterns during winter 2012-13. Under all-sky (cloudy and cloud free) conditions, we find that anthropogenic aerosols over China reduce shortwave radiation reaching the surface by 10-15 Wm^{-2} for most of eastern China; a similar amount of shortwave radiation is absorbed within the atmospheric column as sunlight makes its way through the atmosphere to the surface or is reflected by the surface back to space (Figures S3a, c). Over north-central and northwestern China, aerosols absorb ~5 W m^{-2} of shortwave radiation within the column (Figure S3c). Under clear-sky (i.e., cloud-free) conditions, the impact of aerosol on shortwave radiation reaching the surface nearly doubles while the impact of

aerosols on absorption increases slightly (Figure S3b, d). The remainder of this paper focuses on results under all-sky conditions.

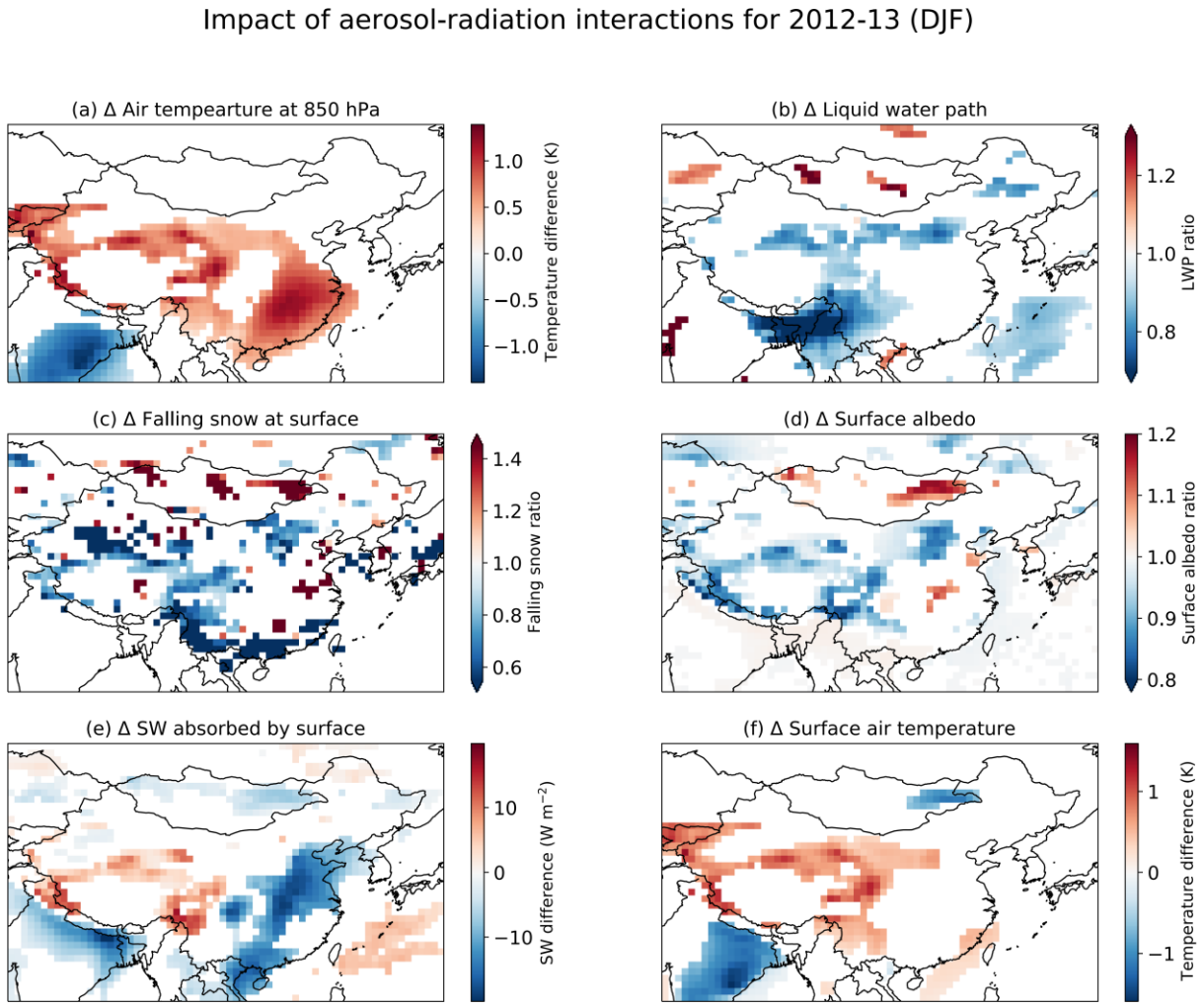

Figure 2: Feedbacks involving aerosol, clouds, snow, and surface albedo. Panels show the impacts of aerosol-radiation interactions during 2012-2013 winter months (DJF) over China on (a) air temperature at 850 hPa, (b) liquid water path (LWP), (c) falling snow at the surface, (d) surface albedo, (e) shortwave radiation (SW) absorbed by the surface, and (f) surface air temperature. Impacts are shown as the difference (a, e, f) or ratio (b, c, d) between the ensemble mean for GEOS-GC and of GEOS-GC-China0. Colored areas indicate those regions where differences are statistically significant ($p < 0.05$).

The absorption by aerosols in the shortwave leads to substantial heating of the lower troposphere (Figure S3e), with an increase in air temperature at 850 hPa of ~0.5-1 K over much of southeastern China, central China, and around the edges of the Tibetan Plateau in winter 2012-13 (Figure 2a). Higher temperatures, in turn, make condensation of cloud liquid water less likely, and the cloud liquid water path is correspondingly reduced near the eastern edge of the Tibetan Plateau and across northern China at ~40°N (Figure 2b). In contrast, cloud liquid water

remains roughly constant in southeastern China, despite the increase in air temperature. The lack of response in cloud liquid water in southeastern China can be traced to relatively high baseline levels of moisture and temperature, which make increases in air temperature less impactful on the already favorable conditions for cloud formation and precipitation compared to cooler and drier regions such as northern China (Figure S4a-d).

We find that aerosol-radiation interactions decrease snowfall at the surface by ~20% near the edges of the Tibetan Plateau and in northeastern and northwestern China in winter 2012-13, with a spatial pattern that roughly aligns with the pattern of decreasing cloud liquid water path (Figure 2c). Snowfall also decreases in southern China, but the small amount of snow in this region makes this change minimal in absolute terms (Figure S4e,f). Snow cover is an important factor in surface albedo in winter, and we find that the reduction in snowfall leads to a decrease in surface albedo of ~5-10% in areas around the Tibetan Plateau and in northeastern China (Figure 2d). In western China, the loss of snow cover increases absorption of shortwave radiation at the surface by ~5-10 Wm^{-2} (Figure 2e). In most of eastern China, however, shortwave radiation absorbed at the surface decreases by ~10-15 Wm^{-2}, driven largely by the attenuation of shortwave radiation by aerosols aloft (Figure S3a). For north-central and parts of northeastern China, absorbed shortwave radiation at the surface changes little, as the effects of decreasing albedo and increasing aerosol reflection and absorption aloft appear to balance out.

Aerosol-radiation interactions in winter 2012-13 increase surface air temperatures in areas bordering the Tibetan Plateau by ~0.5-1 K (Figure 2f). The temperature change is due in large part to the increase in shortwave radiation absorbed at the surface with less snow cover present (Figure 2e). Prevailing westerly winds at the surface and in the lower troposphere carry this relatively warmer air eastward across north-central China (Figure S5a-b), counteracting the surface cooling that would otherwise occur due to the aerosol burden aloft.

GEOS-GC yields a large aerosol burden over the Sichuan Basin, with mean wintertime AOD as much as 1.4 (Figure S6a). We find that the aerosol perturbs regional circulation patterns and affects air temperatures both aloft and at the surface. In the mid- to lower troposphere, regional circulation is dominated by the East Asian winter monsoon (Z. Li et al., 2016), with strong northwesterly winds flowing from the semi-permanent Siberian High and northerly surface winds in eastern China and along the coast (Figure S5). In winter 2012-13, the aerosols over the Sichuan Basin induce a shortwave heating of ~0.5-1 K day^{-1} at 850 hPa (Figure S3c) and ~0.3-0.5 K day^{-1} at 700 hPa (Figure S7a). The East Asian Jet, part of the East Asian monsoon circulation, carries this warm air eastward (Figure S5), causing a local maximum increase in air temperature of ~1.3 K at 850 hPa about 1000 km east of the Basin (Figure 2a). These warmer temperatures lead to a co-located increase in geopotential height of ~70 m at 700 hPa (Figure 3a). Given that geopotential heights over China decrease poleward, this perturbation increases the gradient in geopotential heights just north of ~29° N over eastern China and decreases the gradient south of that, thereby speeding up the East Asian Jet in the north by ~0.5-1 m s^{-1} at 700 hPa but slowing the Jet by ~1 m s^{-1} in the south (Figure 3b). The slowdown in the

south, in turn, exerts drag on winds at lower altitudes, facilitating the flow of warm, marine air into southern China at 850 hPa (Figure 3d) and limiting outflow of pollution at the surface (Figure S5). This weakening of the East Asian monsoon leads to a slight warming of ~0.5 K off the southern coast of China (Figure 2f).

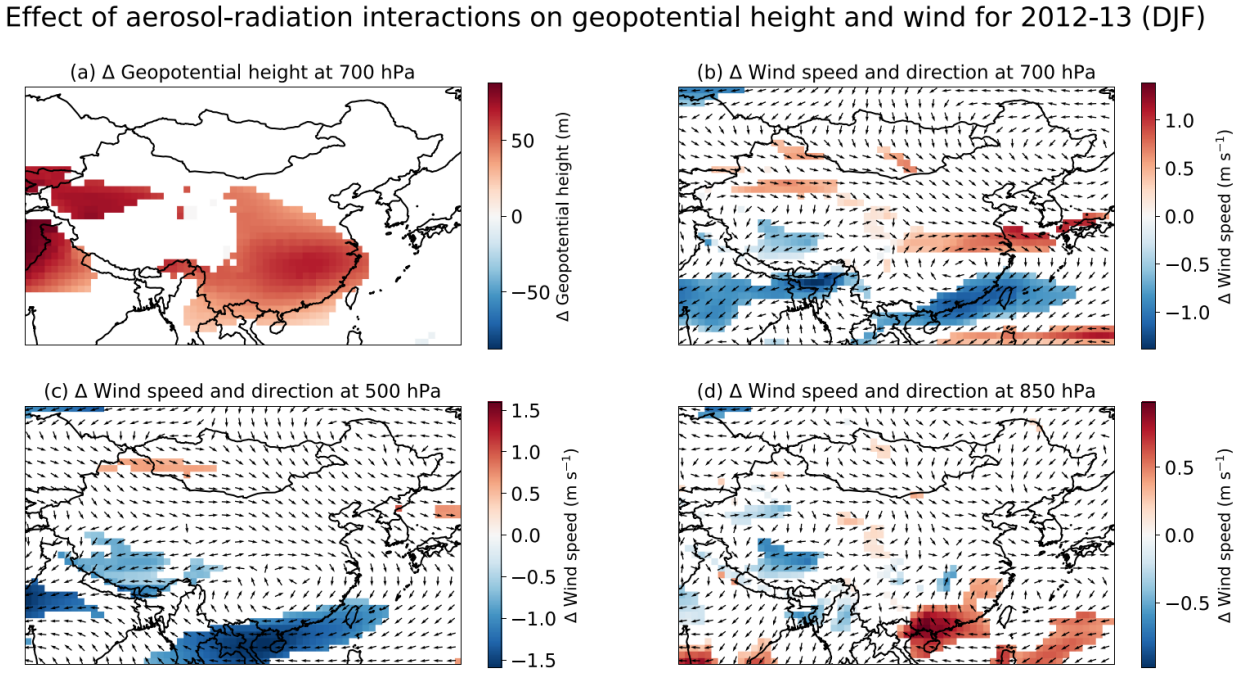

Figure 3: Impact of aerosol-radiation interactions on atmospheric circulation patterns for 2012-2013 in December-January-February (DJF). The panels show the changes in (a) geopotential height and in wind speed and direction at (b) 700 hPa, (c) 500 hPa, and (c) 850 hPa. The impacts are calculated as the difference between the ensemble mean for GEOS-GC and GEOS-GC-China0. Only statistically significant changes ($p < 0.05$) are shown for geopotential height and wind speed. Arrows for (b-c) show the net direction of the wind changes. Blue-shaded regions thus indicate a decrease in wind speed in the opposite direction of the overlying arrows.

Despite the absence of a significant surface temperature response to aerosol-radiation interactions for much of eastern China, the substantial warming of the mid-troposphere in winter 2012-13 nevertheless steepens the vertical potential temperature gradient in the lower troposphere over most of the region, thus enhancing atmospheric stability. Figure 4a shows the effect of aerosol-radiation interactions on lower tropospheric stability (LTS), defined here as the difference in potential temperature at 850 and 1000 hPa (Wood and Bretherton, 2006). We find that LTS increases by ~1 K (10-20%) for most of eastern China south of ~39° N. The increase in LTS reflects a suppression of vertical mixing and decreases PBL heights by ~50 m (~10%) (Figure 4b). Along the eastern and northern edges of the Tibetan Plateau, the surface warming due to the cloud-snowfall-albedo feedback dominates the atmospheric response, resulting in little change in LTS but an increase in PBL height of ~50-100 m. Across the central Tibetan Plateau, a

slowdown in wind speeds in the lower troposphere (Figure 3b,d) reduces overall turbulence and thus PBL height by ~140 m.

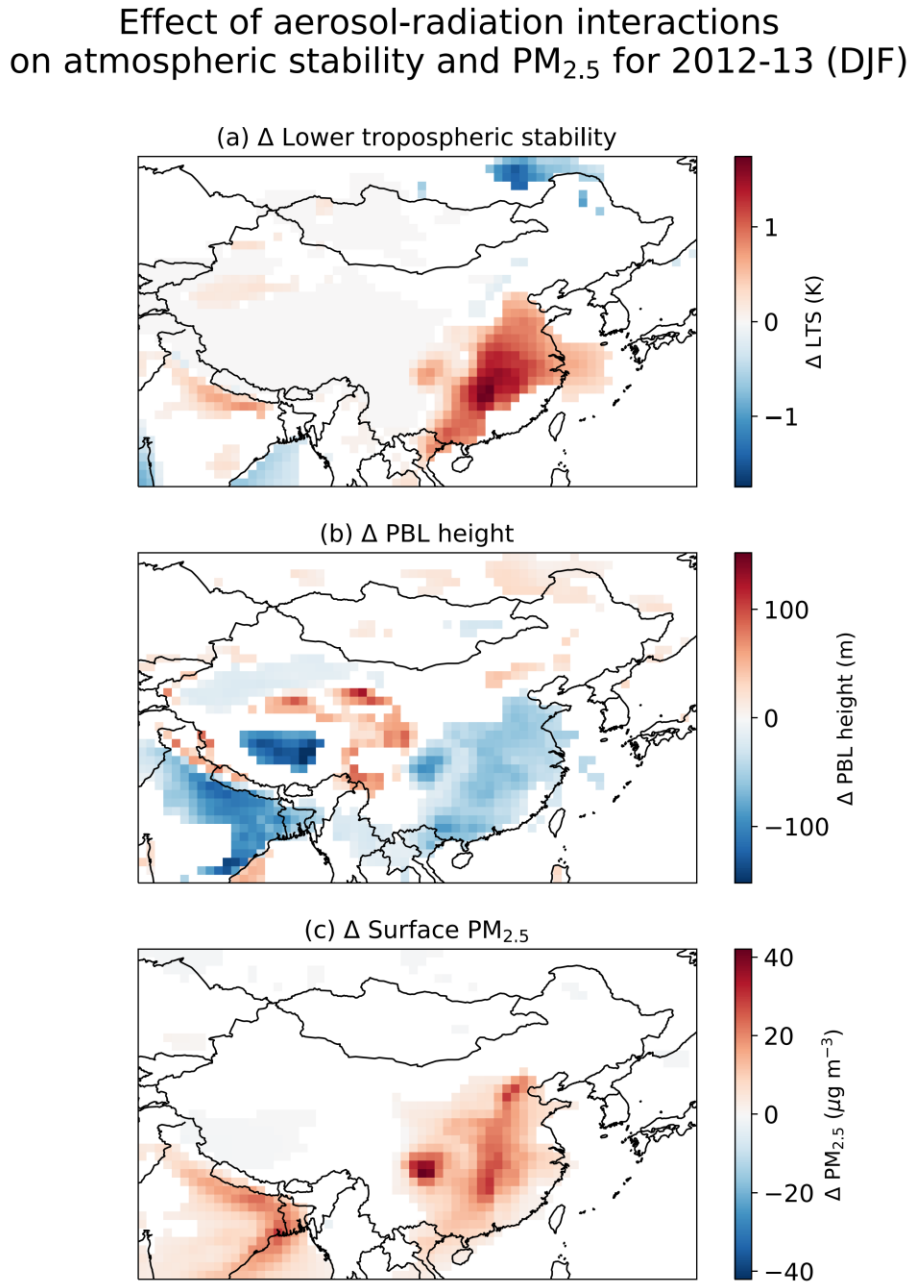

Figure 4: Impact of aerosol-radiation interactions on atmospheric stability and surface $PM_{2.5}$ concentrations. Panel (a) shows the change in lower tropospheric stability, defined as the difference in potential temperature between 850 and 1000 hPa, due to aerosol-radiation interactions; panel (b), the change in planetary boundary layer height; and panel (c), the change in surface $PM_{2.5}$. The impacts are shown as difference between the ensemble mean for GEOS-GC and GEOS-GC-China0. Colored areas indicate those regions where differences are statistically significant changes ($p < 0.05$).

By decreasing PBL height and enhancing stability, we find that aerosol-radiation interactions over China generally limit the volume of air into which surface $PM_{2.5}$ mixes and reduce the vertical dispersion of pollutants. In addition, the aerosol-induced weakening of the East Asian monsoon in southern China reduces ventilation of pollutants. Taken together, these effects lead to an increase in surface $PM_{2.5}$ of ~10-40 μg m^{-3} (~10-20%) across eastern China in winter 2012-13 (Figure 4c). The Sichuan Basin, the region with the highest simulated pollution, shows the largest absolute increase in surface $PM_{2.5}$, ~40 μg m^{-3}. Despite changes in PBL height over the Tibetan Plateau, there is little $PM_{2.5}$ in this region, and so the perturbation in surface $PM_{2.5}$ for this region is minimal.

3.3 Effect of changing emissions on aerosol-radiation interactions and associated impacts

The widespread decrease in $PM_{2.5}$ concentrations between the two periods (2012-13 vs. 2016-17) results in a decline of ~3 W m^{-2} (~5%) in shortwave radiation absorbed by aerosols aloft over eastern China (Figure S8a). This change in shortwave radiation absorption reduces shortwave heating by ~0.1 K day^{-1} (~5-10%) at 850 hPa over eastern China, excluding the southeast (Figure S8b). The decline in shortwave heating of the lower troposphere due to aerosols in 2016-2017 increases snowfall and thus surface albedo in parts of north China, compared to 2012-13 (Figure S8c,d).

In northwestern China, surface dust concentrations increase by ~30% in 2016-17, as discussed below. This increase in dust along with the enhanced surface albedo leads to ~1 W m^{-2} more atmospheric absorption due to aerosol-radiation interactions for 2016-17 compared to 2012-13 (Figure S8a). The presence of anthropogenic aerosols aloft amplifies dust absorption through scattering of incoming sunlight. The aerosol-induced increase in surface albedo, compared to induced reduction in 2012-13, means that more sunlight is reflected back to space, allowing a second pass through the atmosphere. The enhanced absorption increases the aerosol impact on shortwave heating by 0.05 K day^{-1} over northwestern China (Figure S8b).

Across northern China, the cloud-snowfall-albedo feedback weakens in 2016-17, so that aerosols decrease absorption of shortwave radiation at the surface by ~5 W m^{-2} (Figure S9e), a 5-10 W m^{-2} reduction in the aerosol impact relative to 2012-13 (Figure 5a). The weakening of this feedback leads in turn to cooler surface temperatures of ~0.5-1 K in northeastern China in 2016-17 (Figure S9f), ~0.5 K cooler than the impact in 2012-2013 (Figure 5b). The cooling impact in the northeast also leads to a more stable lower troposphere and ~50 m lower PBL heights (Figure 5c, S10a,b).

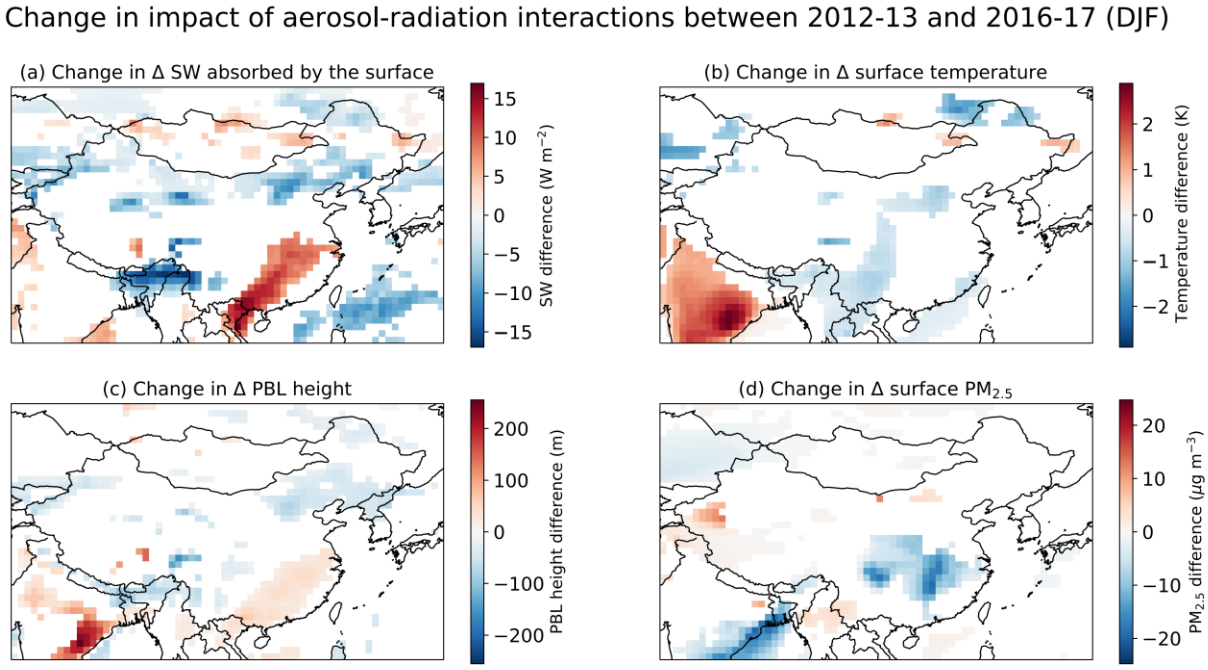

Figure 5: Change in the impacts of aerosol radiation interactions from 2012-13 to 2016-17 (DJF) for (a) shortwave radiation (SW) absorbed by the surface, (b) surface temperature, (c) planetary boundary layer (PBL) height, and (d) surface $PM_{2.5}$ concentrations. All changes are shown as the difference between aerosol-induced effects for 2016-17 versus those effects for 2012-13 – i.e., the differences between the difference of the ensemble means for GEOS-GC and GEOS-GC-China0 in each of the two time periods. Colored areas indicate those regions where differences are statistically significant ($p < 0.05$).

In contrast, over southeastern China in 2016-17, the decline in aerosol aloft increases shortwave radiation absorbed by the surface relative to 2012-13 by ~8-14 W m^{-2} (Figure 5a), resulting in a reduction in 2016-17 of shortwave radiation absorbed by the surface of ~0-5 W m^{-2} (Figure S9e). However, transport of cooler air from the north and west counteracts the local effect of greater absorption of shortwave radiation at the surface, leading to little net change in surface temperatures in 2016-17 (Figure S9f), similar to the impact in the first time period (Figure 5b). The reduced warming attributed to aerosols in the mid- and lower troposphere in conjunction with only minor changes in surface air temperatures leads to an overall decrease in PBL stratification and thus a slight increase of ~50 m in PBL heights (Figure 5c).

Differences in atmospheric circulation patterns over China between winter 2012-13 and winter 2016-17 are likely driven by both changing aerosol load as well as different SSTs applied to the two time periods. We attribute reductions in geopotential heights at 700 hPa by ~25-75 m relative to those in the first period (Figure S11a) to the decline in aerosol-induced heating in the mid- and lower troposphere over most of eastern China in 2016-17 (Figure S8b). This change in geopotential heights allows northerly surface winds associated with the East Asian Winter monsoon to penetrate further south, enhancing the transport of cool air from the north and west

and leading to a relative cooling due to aerosols of ~0.5 K along the southeastern coast of China between the two periods (Figure 5b). The strengthening of the East Asian Monsoon during 2016-17 may partly account for the increased dust mobilization in northwest China, as mentioned above.

The absolute magnitude of the surface $PM_{2.5}$ enhancement due to aerosol-radiation interactions is a function of both meteorological changes and the concentrations of $PM_{2.5}$ absent these meteorological changes. For most of eastern China, we find that surface $PM_{2.5}$ increases by ~5-20 μg m^{-3} due to aerosol-radiation interactions in 2016-17, or about ~5-15 μg m^{-3} less than that in 2012-13 (Figures 5d, S10c). Reduced anthropogenic emissions and an increase in PBL heights in southeastern China account for most of this difference. Nonetheless, the relative enhancement in surface $PM_{2.5}$ due to aerosol-radiation impacts in 2016-17 remains about the same at ~10-20%.

4 Discussion

Our simulations show that aerosol-radiation interactions can significantly enhance surface $PM_{2.5}$ concentrations by 10-40 μg m^{-3}, or 10-20% over much of China during winter. The relative enhancement is similar for both the 2012-13 winters and the 2016-17 winter despite declining emissions of aerosol precursors. Our findings also point to an important role for a cloud-snowfall-albedo feedback in altering local and regional wintertime climate and counteracting the direct effect of reduced shortwave radiation reaching the surface due to aerosol attenuation aloft. This work also represents the first time that aerosols from the detailed chemical mechanism of GEOS-Chem have been fully coupled to the radiation scheme in an ESM, allowing for simultaneous examination of the effect of aerosol-radiation interactions on both climate and air pollution.

Regarding the cloud-snowfall-albedo feedback, we find that atmospheric warming from absorbing aerosols aloft reduces cloud liquid water content in the lower troposphere, which in turn diminishes snowfall and the surface albedo across northern China and around the Tibetan Plateau. This decline in snowfall and surface albedo leads to an unexpected surface warming of ~0.5-1 K in central China in winter 2012-13, counteracting the cooling due to the direct aerosol effect (i.e., reflection or absorption of shortwave radiation by aerosols aloft). Elsewhere in China, this competition between the cloud-snowfall-albedo feedback and the direct aerosol effect leads to little surface temperature change. The heavy aerosol burden still contributes to increased stratification of the planetary boundary layer, but through warming the mid- and lower troposphere rather than through cooling the surface. As the aerosol burden over China declines between the winter months of 2012-2013 and 2016-2017, the cloud-snowfall-albedo feedback diminishes, with the net result that there is little surface temperature response to declining aerosols or even a slight cooling.

Previous studies have pointed to the role of absorbing aerosols in heating the atmosphere and stabilizing the planetary boundary layer in China (e.g., Ding et al., 2016; Miao et al., 2016; X. Wang et al., 2018). To our knowledge, however, prior studies have not detected the cloud-snowfall-albedo feedback which we report here. This oversight may be because these studies primarily focused on short time periods, on a scale of days to weeks (e.g. Zhang et al., 2015; Qiu et al, 2017; H. Wang et al., 2018), which likely limited the impact of aerosol-radiation interactions on seasonal snowfall accumulation and therefore surface albedo. Other studies have reported a significant reduction in cloudiness and precipitation due to absorbing aerosols over China, but have not focused on snowfall in winter (Zuang et al., 2013; Zhuang et al., 2019).

In many ESMs, simpler representations of chemistry than that in GEOS-Chem may not capture the enhancement of secondary $PM_{2.5}$ – e.g., sulfate or nitrate particles – due to aerosol-radiation interactions (e.g., Z. Li et al., 2016; Bartlett et al., 2018). Because such species tend to scatter incoming sunlight, this shortcoming may in turn lead to an underestimate of the shortwave absorption by black carbon and dust, especially during haze events over China (Bi et al., 2014). Some ESMs include treatments of the effect of aerosols on cloud condensation nuclei or the impact of black carbon deposition on snow; consideration of such effects can complicate attribution of modeled changes in precipitation or snow cover (e.g., Jiang et al., 2017; Lin et al., 2018). By focusing just on aerosol-radiation interactions, our study rules out these other pathways as causes for the simulated reductions in snow cover.

With regards to circulation changes in response to aerosol-radiation interactions, our results agree with prior work, which show an enhancement of the East Asian winter monsoon circulation north of ~29° and a reduction to the south of that (Liu et al., 2019). In contrast to Liu et al. (2019), which considers the impacts of aerosol on both radiation and cloud microphysics, we attribute this change solely to the effect of absorbing aerosols, particularly those over the Sichuan Basin, which alters the latitudinal gradient in geopotential height.

Our results show the importance of considering the impacts of aerosols on regional and local climate and meteorology on seasonal timescales. Our model setup, with detailed GEOS-Chem chemistry coupled to the radiation scheme in an ESM, allows us to identify a novel feedback involving aerosol, cloud water, snowfall and surface albedo; this feedback may be difficult to detect with other model configurations – e.g., with fixed meteorological or chemical boundary conditions. Our work further shows that decreasing emissions of aerosol and aerosol precursors – as occurred between 2012-13 and 2016-2017 – might not significantly reduce $PM_{2.5}$ enhancement due to aerosol-radiation interactions, contrary to what might be expected. This work implies that when designing air quality and climate policies, decision makers should consider a broad range of timescales and spatial scales in which chemical and meteorological feedbacks can occur. As absorbing aerosols play an important role in the feedback mechanisms we identify here, our work also suggests that emissions of these aerosols are an important target for policy makers.

A limitation of our work is that it examines only aerosol-radiation interactions. Consideration of the effect of black carbon deposition on snow albedo would likely enhance the reductions in surface albedo that we report here. Alternatively, inclusion of aerosol-cloud interactions, in which aerosols promote cloud formation by serving as cloud condensation nuclei, could dampen the modelled loss of cloud cover due to absorbing aerosols. Nonetheless, using an ESM linked with detailed chemistry, such as that in GEOS-Chem, represents an important direction for understanding the full range of impacts that aerosols can have on local and regional climate and meteorology. Many prior ESM studies have examined the one-way impacts of aerosols on climate (e.g., Shindell et al., 2016; Collins et la., 2017), but the impact of feedbacks between aerosol and meteorology on surface $PM_{2.5}$ concentrations has to date been less frequently considered.

5 Conclusion:

This work represents the first time that the detailed GEOS-Chem chemistry has been fully coupled with the radiation scheme in an ESM. Our approach allows us to examine aerosol-radiation interactions and the subsequent effects on surface $PM_{2.5}$ concentrations during winter months across two two-year periods in China: 2012-13 and 2016-17. We identify a novel cloud-snowfall-albedo feedback, in which absorbing aerosols warm the mid- and lower troposphere, limiting the condensation of cloud liquid water and thereby reducing snowfall, snow cover, and surface albedo. This feedback counteracts the cooling effect of reduced shortwave radiation reaching the surface in the presence of reflecting and absorbing aerosols aloft. Our work shows that aerosol-radiation interactions enhance wintertime surface $PM_{2.5}$ over China by ~10-20%, mainly due to increased lower tropospheric stability and suppressed planetary boundary layer heights. The significant decline in aerosol and aerosol precursor emissions between 2012-13 and 2016-17 weakens the cloud-snowfall-albedo feedback reported here, and thus the emissions decline has little impact on reducing the relative magnitude of the effect of aerosol-radiation interactions on surface $PM_{2.5}$ concentrations. The important role of absorbing aerosols in our simulations suggests that black carbon may be an important target for policy makers seeking to improve air quality. This work shows the potential for new insights to arise from ESMs fully coupled with detailed chemical mechanisms and for examining the impact of aerosol-driven climate change on surface $PM_{2.5}$.

Acknowledgments. This work was funded by the NASA Modeling, Analysis, and Prediction Program (MAP, 80NSSC17K0134), by the Harvard Global Institute, and by the National Science Foundation Graduate Research Fellowship (DGE1144152). Resources supporting the model simulations were provided by the NASA Center for Climate Simulation at the Goddard Space Flight Center (https://www.nccs.nasa.gov/services/discover). Model output is available at: https://dataverse.harvard.edu/privateurl.xhtml?token=21d78069-72c2-4516-850b-2fa5805a8743. The authors thank Mian Chin, Jeff Pierce, and Jack Kodros for helpful discussions.

References:

Alexander, B., Allman, D. J., Amos, H. M., Fairlie, T. D., Dachs, J., Hegg, D. A., & Sletten, R. S. (2012). Isotopic constraints on the formation pathways of sulfate aerosol in the marine boundary layer of the subtropical northeast Atlantic Ocean. *Journal of Geophysical Research: Atmospheres*, *117*(D6), D06304. https://doi.org/10.1029/2011JD016773

Alexander, B., Park, R. J., Jacob, D. J., Li, Q. B., Yantosca, R. M., Savarino, J., et al. (2005). Sulfate formation in sea-salt aerosols: Constraints from oxygen isotopes. *Journal of Geophysical Research: Atmospheres*, *110*(D10), D10307. https://doi.org/10.1029/2004JD005659

Bacmeister, J. T., Suarez, M. J., & Robertson, F. R. (2006). Rain Reevaporation, Boundary Layer–Convection Interactions, and Pacific Rainfall Patterns in an AGCM. *Journal of the Atmospheric Sciences*, *63*(12), 3383–3403. https://doi.org/10.1175/JAS3791.1

Bian, H., Chin, M., Hauglustaine, D. A., Schulz, M., Myhre, G., Bauer, S. E., et al. (2017). Investigation of global particulate nitrate from the AeroCom phase III experiment. *Atmospheric Chemistry and Physics*, *17*(21), 12911–12940. https://doi.org/10.5194/acp-17-12911-2017

Bartlett, R. E., Bollasina, M. A., Booth, B. B. B., Dunstone, N. J., Marenco, F., Messori, G., & Bernie, D. J. (2018). Do differences in future sulfate emission pathways matter for near-term climate? A case study for the Asian monsoon. *Climate Dynamics*, *50*(5), 1863–1880. https://doi.org/10.1007/s00382-017-3726-6

Bi, J., Huang, J., Hu, Z., Holben, B. N., & Guo, Z. (2014). Investigating the aerosol optical and radiative characteristics of heavy haze episodes in Beijing during January of 2013. *Journal of Geophysical Research: Atmospheres*, 2014JD021757. https://doi.org/10.1002/2014JD021757

Cai, W., Li, K., Liao, H., Wang, H., & Wu, L. (2017). Weather conditions conducive to Beijing severe haze more frequent under climate change. *Nature Climate Change*, *7*(4), 257–262. https://doi.org/10.1038/nclimate3249

Che, H., Zhang, X.-Y., Xia, X., Goloub, P., Holben, B., Zhao, H., et al. (2015). Ground-based aerosol climatology of China: aerosol optical depths from the China Aerosol Remote Sensing Network (CARSNET) 2002–2013. *Atmos. Chem. Phys.*, *15*(13), 7619–7652. https://doi.org/10.5194/acp-15-7619-2015

Che, Huizheng, Xia, X., Zhu, J., Wang, H., Wang, Y., Sun, J., et al. (2014). Aerosol optical properties under the condition of heavy haze over an urban site of Beijing, China. *Environmental Science and Pollution Research*, 1–11. https://doi.org/10.1007/s11356-014-3415-5

Chen, Z., Xie, X., Cai, J., Chen, D., Gao, B., He, B., et al. (2018). Understanding meteorological influences on $PM_{2.5}$ concentrations across China: a temporal and spatial perspective.

Atmospheric Chemistry and Physics, *18*(8), 5343–5358. https://doi.org/10.5194/acp-18-5343-2018

Cheng, T., Chen, H., Gu, X., Yu, T., Guo, J., & Guo, H. (2012). The inter-comparison of MODIS, MISR and GOCART aerosol products against AERONET data over China. *Journal of Quantitative Spectroscopy and Radiative Transfer*, *113*(16), 2135–2145. https://doi.org/10.1016/j.jqsrt.2012.06.016

Chin, M., Savoie, D. L., Huebert, B. J., Bandy, A. R., Thornton, D. C., Bates, T. S., et al. (2000). Atmospheric sulfur cycle simulated in the global model GOCART: Comparison with field observations and regional budgets. *Journal of Geophysical Research: Atmospheres*, *105*(D20), 24689–24712. https://doi.org/10.1029/2000JD900385

Chin, M., Ginoux, P., Kinne, S., Torres, O., Holben, B. N., Duncan, B. N., et al. (2002). Tropospheric Aerosol Optical Thickness from the GOCART Model and Comparisons with Satellite and Sun Photometer Measurements. *Journal of the Atmospheric Sciences*, *59*(3), 461–483. https://doi.org/10.1175/1520-0469(2002)059<0461:TAOTFT>2.0.CO;2

Chou, M.-D. (1992). A Solar Radiation Model for Use in Climate Studies. *Journal of the Atmospheric Sciences*, *49*(9), 762–772. https://doi.org/10.1175/1520-0469(1992)049<0762:ASRMFU>2.0.CO;2

Chou, M.-D., & Suarez, M. J. (1994). *An efficient thermal infrared radiation parameterization for use in general circulation models* (NASA Tech. Memorandum No. NASA/TM-1994–104606). Goddard Space Flight Center Greenbelt, Maryland 20771: National Aeronautics and Space Administration.

Cohen, A. J., Brauer, M., Burnett, R., Anderson, H. R., Frostad, J., Estep, K., et al. (2017). Estimates and 25-year trends of the global burden of disease attributable to ambient air pollution: an analysis of data from the Global Burden of Diseases Study 2015. *The Lancet*, *389*(10082), 1907–1918. https://doi.org/10.1016/S0140-6736(17)30505-6

Colarco, P., Silva, A. da, Chin, M., & Diehl, T. (2010). Online simulations of global aerosol distributions in the NASA GEOS-4 model and comparisons to satellite and ground-based aerosol optical depth. *Journal of Geophysical Research: Atmospheres*, *115*(D14). https://doi.org/10.1029/2009JD012820

Colarco, P. S. (2017, June). *Update on the NASA GEOS-5 Aerosol Forecasting and Data Assimilation System*. Retrieved from https://ntrs.nasa.gov/search.jsp?R=20170006600

Collins, W. J., Lamarque, J.-F., Schulz, M., Boucher, O., Eyring, V., Hegglin, M. I., et al. (2017). AerChemMIP: quantifying the effects of chemistry and aerosols in CMIP6. *Geoscientific Model Development*, *10*(2), 585–607. https://doi.org/10.5194/gmd-10-585-2017

Dang, R., & Liao, H. (2019). Severe winter haze days in the Beijing–Tianjin–Hebei region from 1985 to 2017 and the roles of anthropogenic emissions and meteorology. *Atmospheric Chemistry and Physics*, *19*(16), 10801–10816. https://doi.org/10.5194/acp-19-10801-2019

Darmenov, A., & da Silva, A. M. (2015). *The Quick Fire Emissions Dataset (QFED): Documentation of versions 2.1, 2.2 and 2.4* (Technical Report Series on Global Modeling and Data Assimilation, Volume 38 No. NASA/TM–2015–104606). Goddard Space Flight Center Greenbelt, Maryland 20771: National Aeronautics and Space Administration. Retrieved from https://gmao.gsfc.nasa.gov/pubs/docs/Darmenov796.pdf

Ding, A. J., Huang, X., Nie, W., Sun, J. N., Kerminen, V.-M., Petäjä, T., et al. (2016). Enhanced haze pollution by black carbon in megacities in China. *Geophysical Research Letters*, *43*(6), 2016GL067745. https://doi.org/10.1002/2016GL067745

Fairlie, T. D., Jacob, D. J., Dibb, J. E., Alexander, B., Avery, M. A., van Donkelaar, A., & Zhang, L. (2010). Impact of mineral dust on nitrate, sulfate, and ozone in transpacific Asian pollution plumes. *Atmospheric Chemistry and Physics*, *10*(8), 3999–4012. https://doi.org/10.5194/acp-10-3999-2010

Fan, J., Rosenfeld, D., Yang, Y., Zhao, C., Leung, L. R., & Li, Z. (2015). Substantial contribution of anthropogenic air pollution to catastrophic floods in Southwest China. *Geophysical Research Letters*, *42*(14), 2015GL064479. https://doi.org/10.1002/2015GL064479

Feng, X., Lin, H., Fu, T.-M., Sulprizio, M. P., Zhuang, J., Jacob, D. J., et al. (2021). WRF-GC (v2.0): online two-way coupling of WRF (v3.9.1.1) and GEOS-Chem (v12.7.2) for modeling regional atmospheric chemistry-meteorology interactions. *Geoscientific Model Development Discussions*, 1–48. https://doi.org/10.5194/gmd-2020-441

Fountoukis, C., & Nenes, A. (2007). ISORROPIA II: a computationally efficient thermodynamic equilibrium model for K+–Ca2+–Mg2+–NH4+–Na+–SO42−–NO3−–Cl−–H2O aerosols. *Atmos. Chem. Phys.*, *7*(17), 4639–4659. https://doi.org/10.5194/acp-7-4639-2007

Gao, M., Liu, Z., Wang, Y., Lu, X., Ji, D., Wang, L., et al. (2017). Distinguishing the roles of meteorology, emission control measures, regional transport, and co-benefits of reduced aerosol feedbacks in "APEC Blue." *Atmospheric Environment*, *167*, 476–486. https://doi.org/10.1016/j.atmosenv.2017.08.054

Gao, Y., Zhang, M., Liu, Z., Wang, L., Wang, P., Xia, X., et al. (2015). Modeling the feedback between aerosol and meteorological variables in the atmospheric boundary layer during a severe fog–haze event over the North China Plain. *Atmospheric Chemistry and Physics*, *15*(8), 4279–4295. https://doi.org/10.5194/acp-15-4279-2015

Gelaro, R., McCarty, W., Suárez, M. J., Todling, R., Molod, A., Takacs, L., et al. (2017). The Modern-Era Retrospective Analysis for Research and Applications, Version 2 (MERRA-2). *Journal of Climate*, *30*(14), 5419–5454. https://doi.org/10.1175/JCLI-D-16-0758.1

Ginoux, P., Chin, M., Tegen, I., Prospero, J. M., Holben, B., Dubovik, O., & Lin, S.-J. (2001). Sources and distributions of dust aerosols simulated with the GOCART model. *Journal of Geophysical Research: Atmospheres*, *106*(D17), 20255–20273. https://doi.org/10.1029/2000JD000053

Gong, S. L. (2003). A parameterization of sea-salt aerosol source function for sub- and super-micron particles. *Global Biogeochemical Cycles*, *17*(4). https://doi.org/10.1029/2003GB002079

Guenther, A. B., Jiang, X., Heald, C. L., Sakulyanontvittaya, T., Duhl, T., Emmons, L. K., & Wang, X. (2012). The Model of Emissions of Gases and Aerosols from Nature version 2.1 (MEGAN2.1): an extended and updated framework for modeling biogenic emissions. *Geoscientific Model Development*, *5*(6), 1471–1492. https://doi.org/10.5194/gmd-5-1471-2012

Ham, Y.-G., Rienecker, M. M., Suarez, M. J., Vikhliaev, Y., Zhao, B., Marshak, J., et al. (2014). Decadal prediction skill in the GEOS-5 forecast system. *Climate Dynamics*, *42*(1), 1–20. https://doi.org/10.1007/s00382-013-1858-x

Hill, C., DeLuca, C., Balaji, Suarez, M., & Silva, A. D. (2004). The architecture of the Earth System Modeling Framework. *Computing in Science Engineering*, *6*(1), 18–28. https://doi.org/10.1109/MCISE.2004.1255817

Hu, L., Keller, C. A., Long, M. S., Sherwen, T., Auer, B., Silva, A. D., et al. (2018). Global simulation of tropospheric chemistry at 12.5 km resolution: performance and evaluation of the GEOS-Chem chemical module (v10-1) within the NASA GEOS Earth system model (GEOS-5 ESM). *Geoscientific Model Development*, *11*(11), 4603–4620. https://doi.org/10.5194/gmd-11-4603-2018

Huang, X., Wang, Z., & Ding, A. (2018). Impact of Aerosol-PBL Interaction on Haze Pollution: Multiyear Observational Evidences in North China. *Geophysical Research Letters*, *45*(16), 8596–8603. https://doi.org/10.1029/2018GL079239

Jacob, D. J., & Winner, D. A. (2009). Effect of climate change on air quality. *Atmospheric Environment*, *43*(1), 51–63. https://doi.org/10.1016/j.atmosenv.2008.09.051

Jacobson, M. Z., & Kaufman, Y. J. (2006). Wind reduction by aerosol particles. *Geophysical Research Letters*, *33*(24). https://doi.org/10.1029/2006GL027838

Jaeglé, L., Quinn, P. K., Bates, T. S., Alexander, B., & Lin, J.-T. (2011). Global distribution of sea salt aerosols: new constraints from in situ and remote sensing observations. *Atmospheric Chemistry and Physics*, *11*(7), 3137–3157. https://doi.org/10.5194/acp-11-3137-2011

Jaeglé, L., Shah, V., Thornton, J. A., Lopez-Hilfiker, F. D., Lee, B. H., McDuffie, E. E., et al. (2018). Nitrogen Oxides Emissions, Chemistry, Deposition, and Export Over the Northeast United States During the WINTER Aircraft Campaign. *Journal of Geophysical Research: Atmospheres*, *123*(21), 12,368-12,393. https://doi.org/10.1029/2018JD029133

Janssens-Maenhout, G., Crippa, M., Guizzardi, D., Dentener, F., Muntean, M., Pouliot, G., et al. (2015). HTAP_v2.2: a mosaic of regional and global emission grid maps for 2008 and 2010 to study hemispheric transport of air pollution. *Atmospheric Chemistry and Physics*, *15*(19), 11411–11432. https://doi.org/10.5194/acp-15-11411-2015

Ji, D., Li, L., Wang, Y., Zhang, J., Cheng, M., Sun, Y., et al. (2014). The heaviest particulate air-pollution episodes occurred in northern China in January, 2013: Insights gained from observation. *Atmospheric Environment*, *92*, 546–556. https://doi.org/10.1016/j.atmosenv.2014.04.048

Jiang, Y., Yang, X.-Q., Liu, X., Yang, D., Sun, X., Wang, M., et al. (2017). Anthropogenic aerosol effects on East Asian winter monsoon: The role of black carbon-induced Tibetan Plateau warming. *Journal of Geophysical Research: Atmospheres*, *122*(11), 5883–5902. https://doi.org/10.1002/2016JD026237

Keller, C. A., Knowland, K. E., Duncan, B. N., Liu, J., Anderson, D. C., Das, S., et al. (2021). Description of the NASA GEOS Composition Forecast Modeling System GEOS-CF v1.0. *Journal of Advances in Modeling Earth Systems*, *13*(4), e2020MS002413. https://doi.org/10.1029/2020MS002413

Kodros, J. K., & Pierce, J. R. (2017). Important global and regional differences in aerosol cloud-albedo effect estimates between simulations with and without prognostic aerosol microphysics. *Journal of Geophysical Research: Atmospheres*, *122*(7), 4003–4018. https://doi.org/10.1002/2016JD025886

Leung, D. M., Tai, A. P. K., Mickley, L. J., Moch, J. M., Donkelaar, A. van, Shen, L., & Martin, R. V. (2018). Synoptic meteorological modes of variability for fine particulate matter ($PM_{2.5}$) air quality in major metropolitan regions of China. *Atmospheric Chemistry and Physics*, *18*(9), 6733–6748. https://doi.org/10.5194/acp-18-6733-2018

Li, K., Liao, H., Zhu, J., & Moch, J. M. (2016). Implications of RCP emissions on future PM2.5 air quality and direct radiative forcing over China. *Journal of Geophysical Research: Atmospheres*, 2016JD025623. https://doi.org/10.1002/2016JD025623

Li, S., Yu, C., Chen, L., Tao, J., Letu, H., Ge, W., et al. (2016). Inter-comparison of model-simulated and satellite-retrieved componential aerosol optical depths in China. *Atmospheric Environment*, *141*, 320–332. https://doi.org/10.1016/j.atmosenv.2016.06.075

Li, Z., Gu, X., Wang, L., Li, D., Xie, Y., Li, K., et al. (2013). Aerosol physical and chemical properties retrieved from ground-based remote sensing measurements during heavy haze days in

802 Beijing winter. *Atmos. Chem. Phys.*, *13*(20), 10171–10183. https://doi.org/10.5194/acp-13-
803 10171-2013

804 Li, Zhanqing, Lau, W. K.-M., Ramanathan, V., Wu, G., Ding, Y., Manoj, M. G., et al. (2016).
805 Aerosol and monsoon climate interactions over Asia. *Reviews of Geophysics*, *54*(4), 866–929.
806 https://doi.org/10.1002/2015RG000500

807 Li, Zhanqing, Guo, J., Ding, A., Liao, H., Liu, J., Sun, Y., et al. (2017, November). Aerosol and
808 boundary-layer interactions and impact on air quality. *NATIONAL SCIENCE REVIEW*. GREAT
809 CLARENDON ST, OXFORD OX2 6DP, ENGLAND: OXFORD UNIV PRESS.
810 https://doi.org/10.1093/nsr/nwx117

811 Liao, H., Chang, W., & Yang, Y. (2015). Climatic effects of air pollutants over China: A Review.
812 *Advances in Atmospheric Sciences*, *32*(1), 115–139. https://doi.org/10.1007/s00376-014-0013-x

813 Lin, H., Feng, X., Fu, T.-M., Tian, H., Ma, Y., Zhang, L., et al. (2020). WRF-GC (v1.0): online
814 coupling of WRF (v3.9.1.1) and GEOS-Chem (v12.2.1) for regional atmospheric chemistry
815 modeling – Part 1: Description of the one-way model. *Geoscientific Model Development*, *13*(7),
816 3241–3265. https://doi.org/10.5194/gmd-13-3241-2020

817 Lin, L., Xu, Y., Wang, Z., Diao, C., Dong, W., & Xie, S.-P. (2018). Changes in Extreme Rainfall
818 Over India and China Attributed to Regional Aerosol-Cloud Interaction During the Late 20th
819 Century Rapid Industrialization. *Geophysical Research Letters*, *45*(15), 7857–7865.
820 https://doi.org/10.1029/2018GL078308

821 Lin, S.-J. (2004). A "Vertically Lagrangian" Finite-Volume Dynamical Core for Global Models.
822 *Monthly Weather Review*, *132*(10), 2293–2307. https://doi.org/10.1175/1520-
823 0493(2004)132<2293:AVLFDC>2.0.CO;2

824 Liu, H., Jacob, D. J., Bey, I., & Yantosca, R. M. (2001). Constraints from 210Pb and 7Be on wet
825 deposition and transport in a global three-dimensional chemical tracer model driven by
826 assimilated meteorological fields. *Journal of Geophysical Research: Atmospheres*, *106*(D11),
827 12109–12128. https://doi.org/10.1029/2000JD900839

828 Liu, Q., Jia, X., Quan, J., Li, J., Li, X., Wu, Y., et al. (2018). New positive feedback mechanism
829 between boundary layer meteorology and secondary aerosol formation during severe haze events.
830 *Scientific Reports*, *8*(1), 1–8. https://doi.org/10.1038/s41598-018-24366-3

831 Liu, Z., Ming, Y., Wang, L., Bollasina, M., Luo, M., Lau, N.-C., & Yim, S. H.-L. (2019). A
832 Model Investigation of Aerosol-Induced Changes in the East Asian Winter monsoon.
833 *Geophysical Research Letters*, *46*(16), 10186–10195. https://doi.org/10.1029/2019GL084228

834 Lock, A. P., Brown, A. R., Bush, M. R., Martin, G. M., & Smith, R. N. B. (2000). A New
835 Boundary Layer Mixing Scheme. Part I: Scheme Description and Single-Column Model Tests.

Monthly Weather Review, *128*(9), 3187–3199. https://doi.org/10.1175/1520-0493(2000)128<3187:ANBLMS>2.0.CO;2

Lohmann, U., & Feichter, J. (2005). Global indirect aerosol effects: a review. *Atmospheric Chemistry and Physics*, *5*(3), 715–737. https://doi.org/10.5194/acp-5-715-2005

Long, M. S., Yantosca, R., Nielsen, J. E., Keller, C. A., da Silva, A., Sulprizio, M. P., et al. (2015). Development of a grid-independent GEOS-Chem chemical transport model (v9-02) as an atmospheric chemistry module for Earth system models. *Geosci. Model Dev.*, *8*(3), 595–602. https://doi.org/10.5194/gmd-8-595-2015

Louis, J.-F., Tiedtke, M., & Geleyn, J.-F. (1982). A short history of the PBL parameterization at ECMWF. In *Workshop on Planetary Boundary Layer parameterization, 25-27 November 1981* (pp. 59–79). Shinfield Park, Reading: ECMWF. Retrieved from https://www.ecmwf.int/node/10845

Lu, X., Zhang, L., Wu, T., Long, M. S., Wang, J., Jacob, D. J., et al. (2020). Development of the global atmospheric chemistry general circulation model BCC-GEOS-Chem v1.0: model description and evaluation. *Geoscientific Model Development*, *13*(9), 3817–3838. https://doi.org/10.5194/gmd-13-3817-2020

Luo, G., Yu, F., & Schwab, J. (2019). Revised treatment of wet scavenging processes dramatically improves GEOS-Chem 12.0.0 simulations of surface nitric acid, nitrate, and ammonium over the United States. *Geoscientific Model Development*, *12*(8), 3439–3447. https://doi.org/10.5194/gmd-12-3439-2019

McGrath-Spangler, E. L., & Molod, A. (2014). Comparison of GEOS-5 AGCM planetary boundary layer depths computed with various definitions. *Atmospheric Chemistry and Physics*, *14*(13), 6717–6727. https://doi.org/10.5194/acp-14-6717-2014

Miao, Y., Liu, S., Zheng, Y., & Wang, S. (2016). Modeling the feedback between aerosol and boundary layer processes: a case study in Beijing, China. *Environmental Science and Pollution Research*, *23*(4), 3342–3357. https://doi.org/10.1007/s11356-015-5562-8

Miao, Y., Li, J., Miao, S., Che, H., Wang, Y., Zhang, X., et al. (2019). Interaction Between Planetary Boundary Layer and PM2.5 Pollution in Megacities in China: a Review. *Current Pollution Reports*, *5*(4), 261–271. https://doi.org/10.1007/s40726-019-00124-5

Mickley, L. J., Leibensperger, E. M., Jacob, D. J., & Rind, D. (2012). Regional warming from aerosol removal over the United States: Results from a transient 2010–2050 climate simulation. *Atmospheric Environment*, *46*, 545–553. https://doi.org/10.1016/j.atmosenv.2011.07.030

Moch, J. M., Dovrou, E., Mickley, L. J., Keutsch, F. N., Cheng, Y., Jacob, D. J., et al. (2018). Contribution of Hydroxymethane Sulfonate to Ambient Particulate Matter: A Potential

Explanation for High Particulate Sulfur During Severe Winter Haze in Beijing. *Geophysical Research Letters*, *45*(21), 11,969-11,979. https://doi.org/10.1029/2018GL079309

Moch, J. M., Dovrou, E., Mickley, L. J., Keutsch, F. N., Liu, Z., Wang, Y., et al. (2020). Global Importance of Hydroxymethanesulfonate in Ambient Particulate Matter: Implications for Air Quality. *Journal of Geophysical Research: Atmospheres*, *125*(18), e2020JD032706. https://doi.org/10.1029/2020JD032706

Moch, J. M. (2020). Investigating the Chemical and Climatic Mechanisms Driving Extreme Air Pollution Episodes. Retrieved from https://dash.harvard.edu/handle/1/37365746

Molod, A., Takacs, L., Suarez, M., & Bacmeister, J. (2015). Development of the GEOS-5 atmospheric general circulation model: evolution from MERRA to MERRA-2. *Geoscientific Model Development*, *8*(5), 1339–1356. https://doi.org/10.5194/gmd-8-1339-2015

Molod, Andrea, Takacs, L., Suárez, M. J., Bacmeister, J., Song, I.-S., & Eichmann, A. (2012). *The GEOS-5 Atmospheric General Circulation Model: Mean Climate and Development from MERRA to Fortuna* (Technical Report Series on Global Modeling and Data Assimilation, Volume 28 No. NASA/TM–2012-104606). Goddard Space Flight Center Greenbelt, Maryland 20771: National Aeronautics and Space Administration. Retrieved from https://gmao.gsfc.nasa.gov/pubs/docs/tm28.pdf

Molod, Andrea, Hackert, E., Vikhliaev, Y., Zhao, B., Barahona, D., Vernieres, G., et al. (2020). GEOS-S2S Version 2: The GMAO High-Resolution Coupled Model and Assimilation System for Seasonal Prediction. *Journal of Geophysical Research: Atmospheres*, *125*(5), e2019JD031767. https://doi.org/10.1029/2019JD031767

Moorthi, S., & Suarez, M. J. (1992). Relaxed Arakawa-Schubert. A Parameterization of Moist Convection for General Circulation Models. *Monthly Weather Review*, *120*(6), 978–1002. https://doi.org/10.1175/1520-0493(1992)120<0978:RASAPO>2.0.CO;2

Morgenstern, O., Hegglin, M. I., Rozanov, E., O'Connor, F. M., Abraham, N. L., Akiyoshi, H., et al. (2017). Review of the global models used within phase 1 of the Chemistry–Climate Model Initiative (CCMI). *Geoscientific Model Development*, *10*(2), 639–671. https://doi.org/10.5194/gmd-10-639-2017

Myhre, G., Shindell, D., Bréon, F., Collins, W., Fuglestvedt, J., Huang, J., et al. (2013). Anthropogenic and Natural Radiative Forcing. In T. Stocker (Ed.), *Climate change 2013: the physical science basis; Working Group I contribution to the fifth assessment report of the Intergovernmental Panel on Climate Change*. Cambridge University Press. https://doi.org/10.1017/CBO9781107415324.018

Nielsen, J. E., Pawson, S., Molod, A., Auer, B., da Silva, A. M., Douglass, A. R., et al. (2017). Chemical Mechanisms and Their Applications in the Goddard Earth Observing System (GEOS)

Earth System Model. *Journal of Advances in Modeling Earth Systems*, *9*(8), 3019–3044. https://doi.org/10.1002/2017MS001011

Niu, F., Li, Z., Li, C., Lee, K.-H., & Wang, M. (2018). Increase of wintertime fog in China: Potential impacts of weakening of the Eastern Asianmonsoon circulation and increasing aerosol loading. *Journal of Geophysical Research: Atmospheres*. https://doi.org/10.1029/2009JD013484@10.1002/(ISSN)2169-8996.EASTAIRC1

Orbe, C., Oman, L. D., Strahan, S. E., Waugh, D. W., Pawson, S., Takacs, L. L., & Molod, A. M. (2017). Large-Scale Atmospheric Transport in GEOS Replay Simulations. *Journal of Advances in Modeling Earth Systems*, *9*(7), 2545–2560. https://doi.org/10.1002/2017MS001053

Pai, S. J., Heald, C. L., Pierce, J. R., Farina, S. C., Marais, E. A., Jimenez, J. L., et al. (2020). An evaluation of global organic aerosol schemes using airborne observations. *Atmospheric Chemistry and Physics*, *20*(5), 2637–2665. https://doi.org/10.5194/acp-20-2637-2020

Park, R. J., Jacob, D. J., Field, B. D., Yantosca, R. M., & Chin, M. (2004). Natural and transboundary pollution influences on sulfate-nitrate-ammonium aerosols in the United States: Implications for policy. *Journal of Geophysical Research: Atmospheres*, *109*(D15), D15204. https://doi.org/10.1029/2003JD004473

Philip, S., Martin, R. V., Snider, G., Weagle, C. L., Donkelaar, A. van, Brauer, M., et al. (2017). Anthropogenic fugitive, combustion and industrial dust is a significant, underrepresented fine particulate matter source in global atmospheric models. *Environmental Research Letters*, *12*(4), 044018. https://doi.org/10.1088/1748-9326/aa65a4

Putman, W. M., & Lin, S.-J. (2007). Finite-volume transport on various cubed-sphere grids. *Journal of Computational Physics*, *227*(1), 55–78. https://doi.org/10.1016/j.jcp.2007.07.022

Pye, H. O. T., Liao, H., Wu, S., Mickley, L. J., Jacob, D. J., Henze, D. K., & Seinfeld, J. H. (2009). Effect of changes in climate and emissions on future sulfate-nitrate-ammonium aerosol levels in the United States. *Journal of Geophysical Research: Atmospheres*, *114*(D1). https://doi.org/10.1029/2008JD010701

Qiu, Y., Liao, H., Zhang, R., & Hu, J. (2017). Simulated impacts of direct radiative effects of scattering and absorbing aerosols on surface layer aerosol concentrations in China during a heavily polluted event in February 2014. *Journal of Geophysical Research: Atmospheres*, *122*(11), 5955–5975. https://doi.org/10.1002/2016JD026309

Quan, J., Tie, X., Zhang, Q., Liu, Q., Li, X., Gao, Y., & Zhao, D. (2014). Characteristics of heavy aerosol pollution during the 2012–2013 winter in Beijing, China. *Atmospheric Environment*, *88*, 83–89. https://doi.org/10.1016/j.atmosenv.2014.01.058

Rienecker, M., Suarez, M. J., Todling, R., Bacmeister, J., Takacs, L., Liu, H.-C., et al. (2008). *The GEOS-5 Data Assimilation System—Documentation of Versions 5.0.1, 5.1.0, and 5.2.0* (Technical Report Series on Global Modeling and Data Assimilation, Volume 27 No. NASA/TM–2008–104606). Goddard Space Flight Center Greenbelt, Maryland 20771: National Aeronautics and Space Administration. Retrieved from https://gmao.gsfc.nasa.gov/pubs/docs/tm27.pdf

Shah, V., Jacob, D. J., Li, K., Silvern, R. F., Zhai, S., Liu, M., et al. (2020). Effect of changing NO_x lifetime on the seasonality and long-term trends of satellite-observed tropospheric NO_2 columns over China. *Atmospheric Chemistry and Physics*, *20*(3), 1483–1495. https://doi.org/10.5194/acp-20-1483-2020

Shao, J., Chen, Q., Wang, Y., Lu, X., He, P., Sun, Y., et al. (2019). Heterogeneous sulfate aerosol formation mechanisms during wintertime Chinese haze events: air quality model assessment using observations of sulfate oxygen isotopes in Beijing. *Atmospheric Chemistry and Physics*, *19*(9), 6107–6123. https://doi.org/10.5194/acp-19-6107-2019

Sherwen, T., Schmidt, J. A., Evans, M. J., Carpenter, L. J., Großmann, K., Eastham, S. D., et al. (2016). Global impacts of tropospheric halogens (Cl, Br, I) on oxidants and composition in GEOS-Chem. *Atmospheric Chemistry and Physics*, *16*(18), 12239–12271. https://doi.org/10.5194/acp-16-12239-2016

Shindell, D. T., Lee, Y., & Faluvegi, G. (2016). Climate and health impacts of US emissions reductions consistent with 2 °C. *Nature Climate Change*, *6*(5), 503–507. https://doi.org/10.1038/nclimate2935

Simmons, A. J., & Burridge, D. M. (1981). An Energy and Angular-Momentum Conserving Vertical Finite-Difference Scheme and Hybrid Vertical Coordinates. *Monthly Weather Review*, *109*(4), 758–766. https://doi.org/10.1175/1520-0493(1981)109<0758:AEAAMC>2.0.CO;2

Tokioka, T., Yamazaki, K., Kitoh, A., & Ose, T. (1988). The equatorial 30-60 day oscillation and the Arakawa-Schubert penetrative cumulus parameterization. *The Equatorial 30-60 Day Oscillation and the Arakawa-Schubert Penetrative Cumulus Parameterization*, *66*(6), 883–901.

Travis, K. R., Jacob, D. J., Fisher, J. A., Kim, P. S., Marais, E. A., Zhu, L., et al. (2016). Why do models overestimate surface ozone in the Southeast United States? *Atmospheric Chemistry and Physics*, *16*(21), 13561–13577. https://doi.org/10.5194/acp-16-13561-2016

van der Werf, G. R., Randerson, J. T., Giglio, L., Leeuwen, T. T. van, Chen, Y., Rogers, B. M., et al. (2017). Global fire emissions estimates during 1997–2016. *Earth System Science Data*, *9*(2), 697–720. https://doi.org/10.5194/essd-9-697-2017

Vohra, K., Vodonos, A., Schwartz, J., Marais, E. A., Sulprizio, M. P., & Mickley, L. J. (2021). Global mortality from outdoor fine particle pollution generated by fossil fuel combustion:

Results from GEOS-Chem. *Environmental Research*, *195*, 110754. https://doi.org/10.1016/j.envres.2021.110754

Wang, C., An, X., Zhang, P., Sun, Z., Cui, M., & Ma, L. (2019). Comparing the impact of strong and weak East Asian wintermonsoon on PM2.5 concentration in Beijing. *Atmospheric Research*, *215*, 165–177. https://doi.org/10.1016/j.atmosres.2018.08.022

Wang, H., Peng, Y., Zhang, X., Liu, H., Zhang, M., Che, H., et al. (2018). Contributions to the explosive growth of $PM_{2.5}$ mass due to aerosol–radiation feedback and decrease in turbulent diffusion during a red alert heavy haze in Beijing–Tianjin–Hebei, China. *Atmospheric Chemistry and Physics*, *18*(23), 17717–17733. https://doi.org/10.5194/acp-18-17717-2018

Wang, J., Wang, S., Jiang, J., Ding, A., Zheng, M., Zhao, B., et al. (2014). Impact of aerosol–meteorology interactions on fine particle pollution during China's severe haze episode in January 2013. *Environmental Research Letters*, *9*(9), 094002. https://doi.org/10.1088/1748-9326/9/9/094002

Wang, Q., Jacob, D. J., Spackman, J. R., Perring, A. E., Schwarz, J. P., Moteki, N., et al. (2014). Global budget and radiative forcing of black carbon aerosol: Constraints from pole-to-pole (HIPPO) observations across the Pacific. *Journal of Geophysical Research: Atmospheres*, *119*(1), 2013JD020824. https://doi.org/10.1002/2013JD020824

Wang, X., He, X., Miao, S., & Dou, Y. (2018). Numerical simulation of the influence of aerosol-radiation effect on urban boundary layer. *Science China Earth Sciences*, *61*(12), 1844–1858. https://doi.org/10.1007/s11430-018-9260-0

Wang, Y., Wang, M., Zhang, R., Ghan, S. J., Lin, Y., Hu, J., et al. (2014). Assessing the effects of anthropogenic aerosols on Pacific storm track using a multiscale global climate model. *Proceedings of the National Academy of Sciences*, *111*(19), 6894–6899. https://doi.org/10.1073/pnas.1403364111

Wood, R., & Bretherton, C. S. (2006). On the Relationship between Stratiform Low Cloud Cover and Lower-Tropospheric Stability. *Journal of Climate*, *19*(24), 6425–6432. https://doi.org/10.1175/JCLI3988.1

Wu, G., Li, Z., Fu, C., Zhang, X., Zhang, R., Zhang, R., et al. (2016). Advances in studying interactions between aerosols and monsoon in China. *Science China Earth Sciences*, *59*(1), 1–16. https://doi.org/10.1007/s11430-015-5198-z

Wu, S., Mickley, L. J., Jacob, D. J., Logan, J. A., Yantosca, R. M., & Rind, D. (2007). Why are there large differences between models in global budgets of tropospheric ozone? *Journal of Geophysical Research: Atmospheres*, *112*(D5). https://doi.org/10.1029/2006JD007801

Xia, X., Che, H., Zhu, J., Chen, H., Cong, Z., Deng, X., et al. (2016). Ground-based remote sensing of aerosol climatology in China: Aerosol optical properties, direct radiative effect and its parameterization. *Atmospheric Environment*, *124*, *Part B*, 243–251. https://doi.org/10.1016/j.atmosenv.2015.05.071

Xie, Y., Li, Z., Li, D., Xu, H., & Li, K. (2015). Aerosol Optical and Microphysical Properties of Four Typical Sites of SONET in China Based on Remote Sensing Measurements. *Remote Sensing*, *7*(8), 9928–9953. https://doi.org/10.3390/rs70809928

Yu, K., Keller, C. A., Jacob, D. J., Molod, A. M., Eastham, S. D., & Long, M. S. (2018). Errors and improvements in the use of archived meteorological data for chemical transport modeling: an analysis using GEOS-Chem v11-01 driven by GEOS-5 meteorology. *Geoscientific Model Development*, *11*(1), 305–319. https://doi.org/10.5194/gmd-11-305-2018

Zhai, S., Jacob, D. J., Wang, X., Shen, L., Li, K., Zhang, Y., et al. (2019). Fine particulate matter (PM2.5) trends in China, 2013–2018: separating contributions from anthropogenic emissions and meteorology. *Atmos. Chem. Phys.*, *19*(16), 11031–11041. https://doi.org/10.5194/acp-19-11031-2019

Zhai, S., Jacob, D. J., Wang, X., Liu, Z., Wen, T., Shah, V., et al. (2021). Control of particulate nitrate air pollution in China. *Nature Geoscience*, *14*(6), 389–395. https://doi.org/10.1038/s41561-021-00726-z

Zhang, B., Wang, Y., & Hao, J. (2015). Simulating aerosol–radiation–cloud feedbacks on meteorology and air quality over eastern China under severe haze conditionsin winter. *Atmospheric Chemistry and Physics*, *15*(5), 2387–2404. https://doi.org/10.5194/acp-15-2387-2015

Zhang, H., Wang, Z., Wang, Z., Liu, Q., Gong, S., Zhang, X., et al. (2012). Simulation of direct radiative forcing of aerosols and their effects on East Asian climate using an interactive AGCM-aerosol coupled system. *Climate Dynamics*, *38*(7), 1675–1693. https://doi.org/10.1007/s00382-011-1131-0

Zhang, Leiming, Gong, S., Padro, J., & Barrie, L. (2001). A size-segregated particle dry deposition scheme for an atmospheric aerosol module. *Atmospheric Environment*, *35*(3), 549–560. https://doi.org/10.1016/S1352-2310(00)00326-5

Zhang, Q., Zheng, Y., Tong, D., Shao, M., Wang, S., Zhang, Y., et al. (2019). Drivers of improved $PM_{2.5}$ air quality in China from 2013 to 2017. *Proceedings of the National Academy of Sciences*, *116*(49), 24463. https://doi.org/10.1073/pnas.1907956116

Zhang, X., Wang, H., Che, H.-Z., Tan, S.-C., Shi, G.-Y., & Yao, X.-P. (2020). The impact of aerosol on MODIS cloud detection and property retrieval in seriously polluted East China. *Science of The Total Environment*, *711*, 134634. https://doi.org/10.1016/j.scitotenv.2019.134634

Zheng, B., Tong, D., Li, M., Liu, F., Hong, C., Geng, G., et al. (2018). Trends in China's anthropogenic emissions since 2010 as the consequence of clean air actions. *Atmospheric Chemistry and Physics*, *18*(19), 14095–14111. https://doi.org/10.5194/acp-18-14095-2018

Zheng, G. J., Duan, F. K., Su, H., Ma, Y. L., Cheng, Y., Zheng, B., et al. (2015). Exploring the severe winter haze in Beijing: the impact of synoptic weather, regional transport and heterogeneous reactions. *Atmos. Chem. Phys.*, *15*(6), 2969–2983. https://doi.org/10.5194/acp-15-2969-2015

Zhong, J., Zhang, X., Dong, Y., Wang, Y., Liu, C., Wang, J., et al. (2018a). Feedback effects of boundary-layer meteorological factors on cumulative explosive growth of $PM_{2.5}$ during winter heavy pollution episodes in Beijing from 2013 to 2016. *Atmospheric Chemistry and Physics*, *18*(1), 247–258. https://doi.org/10.5194/acp-18-247-2018

Zhong, J., Zhang, X., Wang, Y., Liu, C., & Dong, Y. (2018b). Heavy aerosol pollution episodes in winter Beijing enhanced by radiative cooling effects of aerosols. *Atmospheric Research*, *209*, 59–64. https://doi.org/10.1016/j.atmosres.2018.03.011

Zhong, J., Zhang, X., Wang, Y., Wang, J., Shen, X., Zhang, H., et al. (2019). The two-way feedback mechanism between unfavorable meteorological conditions and cumulative aerosol pollution in various haze regions of China. *Atmospheric Chemistry and Physics*, *19*(5), 3287–3306. https://doi.org/10.5194/acp-19-3287-2019

Zhou, M., Zhang, L., Chen, D., Gu, Y., Fu, T.-M., Gao, M., et al. (2019). The impact of aerosol–radiation interactions on the effectiveness of emission control measures. *Environmental Research Letters*, *14*(2), 024002. https://doi.org/10.1088/1748-9326/aaf27d

Zhuang, B., Liu, Q., Wang, T., Yin, C., Li, S., Xie, M., et al. (2013). Investigation on semi-direct and indirect climate effects of fossil fuel black carbon aerosol over China. *Theoretical and Applied Climatology*, *114*(3), 651–672. https://doi.org/10.1007/s00704-013-0862-8

Zhuang, B. L., Chen, H. M., Li, S., Wang, T. J., Liu, J., Zhang, L. J., et al. (2019). The direct effects of black carbon aerosols from different source sectors in East Asia in summer. *Climate Dynamics*, *53*(9), 5293–5310. https://doi.org/10.1007/s00382-019-04863-5